Wear of Metal Forming Dies

Huseyin CIMENOGLU

Department of Metallurgical and Materials Engineering
Istanbul Technical University

17.04.2026

Metal Forming Operations

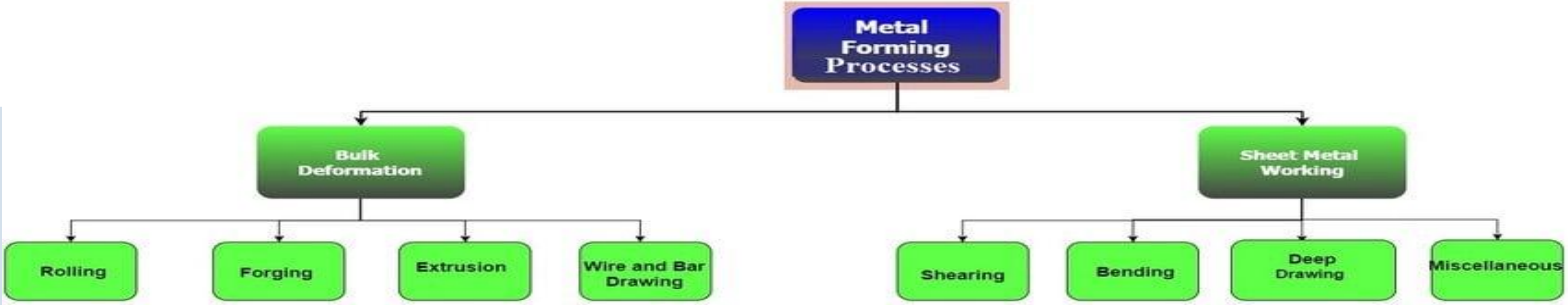

- The surface area to volume of the work is relatively small,
- Severe plastic deformation process resulting in massive shape change,
- Plastic deformation takes place by the compressive stresses,
- Temperature > 0.5 Tm (K). For steels temperature can get up to 1150 °C

- The surface area to volume of the work is relatively high
- Involves forming and cutting operations on metal sheets via tensile and shear stresses.
- Temperarature < 0.3 Tm (K). For steels temperature less than 200 °C

https://doi.org/10.13140/RG.2.2.18467.43049

https://insights.globalspec.com/article/11169/metal-forming-machine-tools-part-1-bulk-metal

https://www.linkedin.com/posts/mechanicalcaddacademy_sheetmetal-metalforming-mechanicalengineering-activity-7317420282615365632-51q6

Die / Workpeice Contact During Forming Operations

Example of Hot Forging

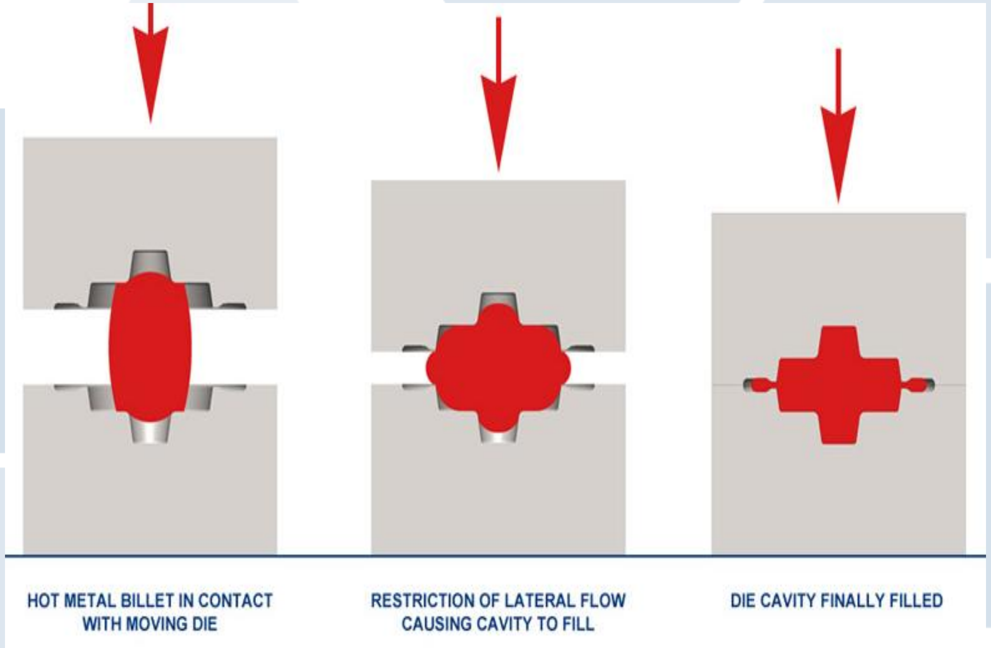

https://metallurgicalresources.com/making-closed-die-forged-parts/

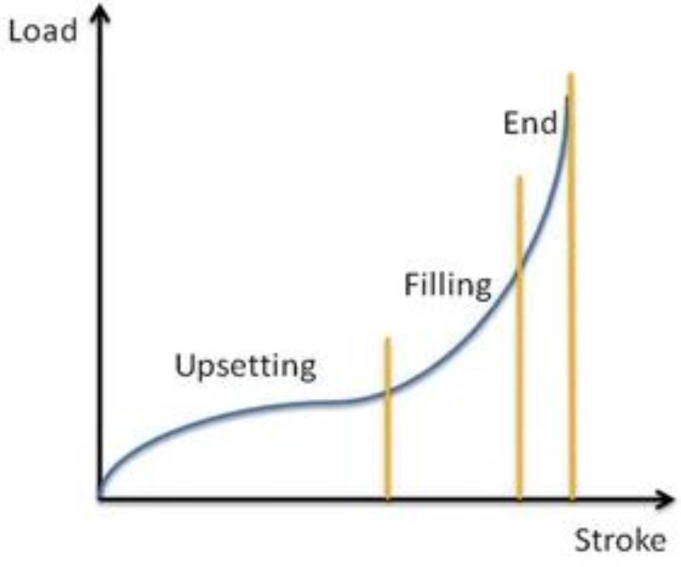

https://doi.org/10.1007/978-1-4471-4976-7_44-31

<u>Friction and constraint</u>

Interface friction, flash formation, and die cavity constraints can push required pressure to 2–4 X the flow stress.

Tribo-Contact at Die / Workpiece Interface

Example of Hot Forging

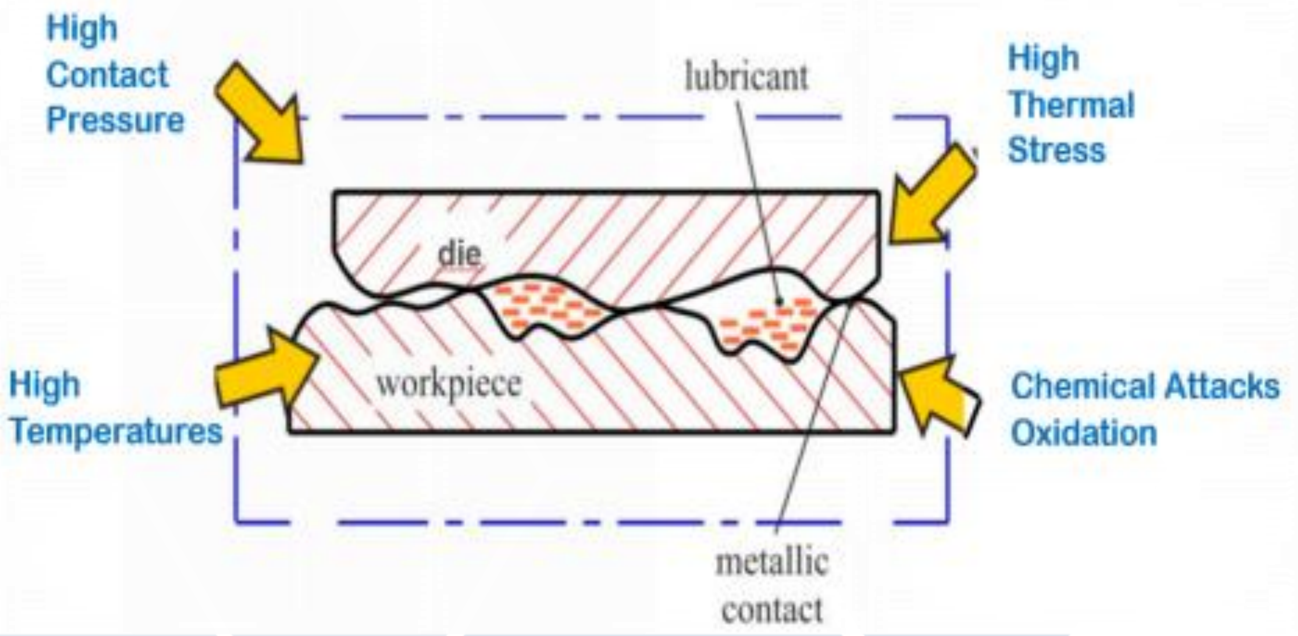

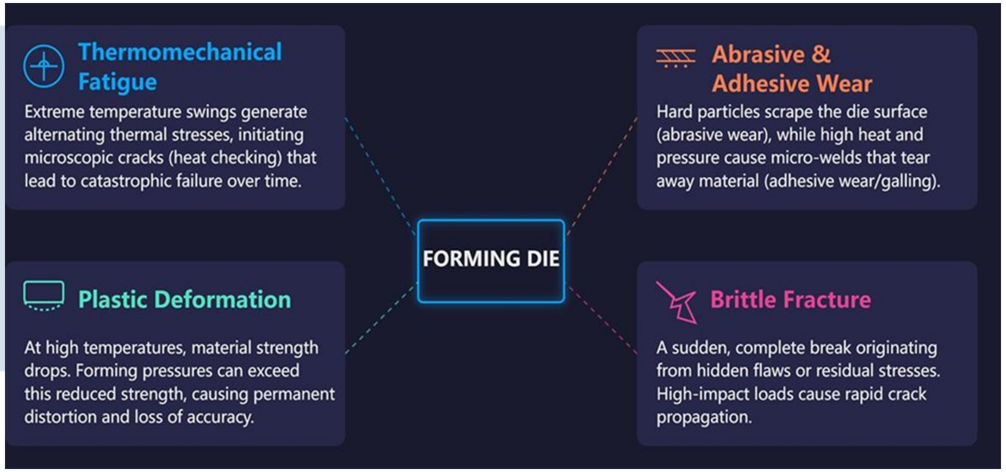

https://www.jeelix.com/metal-forming-die-materials-selection-criteria/

Die surfaces experience:

Impact and Sliding Contacts

Contact Pressure >> 1 GPa

Failure of Forging Dies

Failure mechanisms

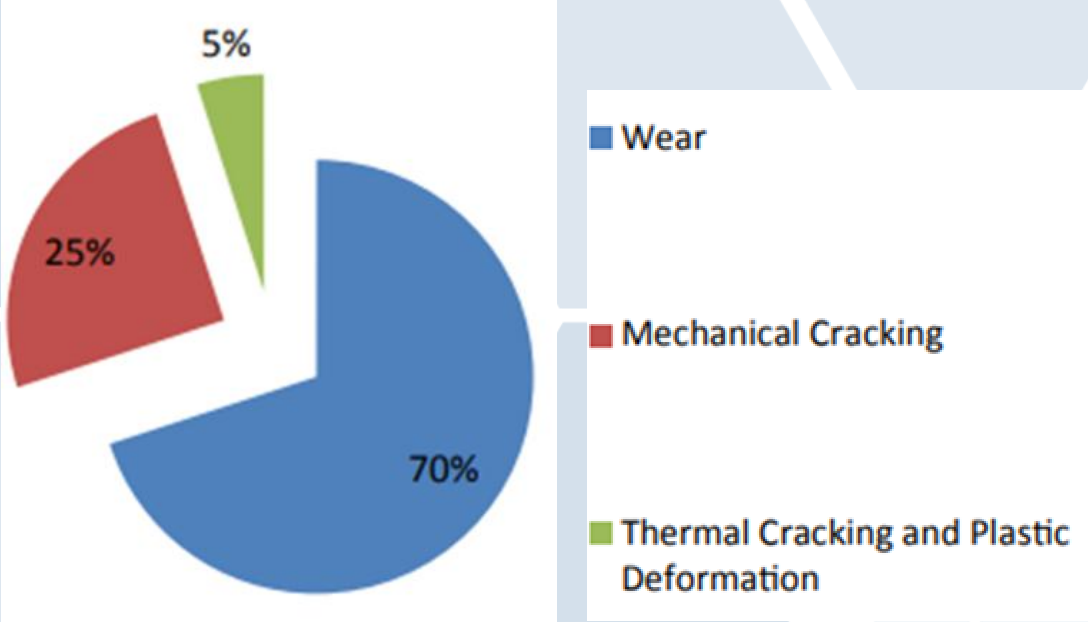

A. Emamverdian , Y. Sun, C. Cao, .C. Prunc, Y. Wang, Engineering Failure Analysis 129 2021, 105678

Wear mechanisms

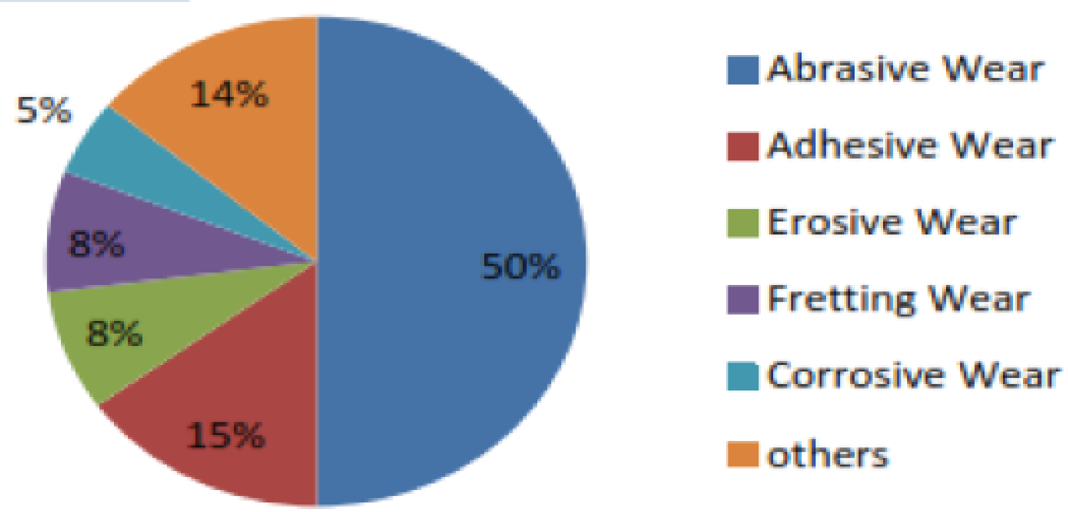

S.Chandera and V. Chawla, Materials Today: Proceedings 4 (2017) 1147–1157

Steels for Die Manufacturing

- **Dies are manufactured from high-carbon and high alloyed steels (> 10wt%)**
- **Inclusions and impurities are tightly controlled.**
- **They are classified as Die Steels or Tool Steels**
- **They are used after Q&T for high hardness and wear resistance**

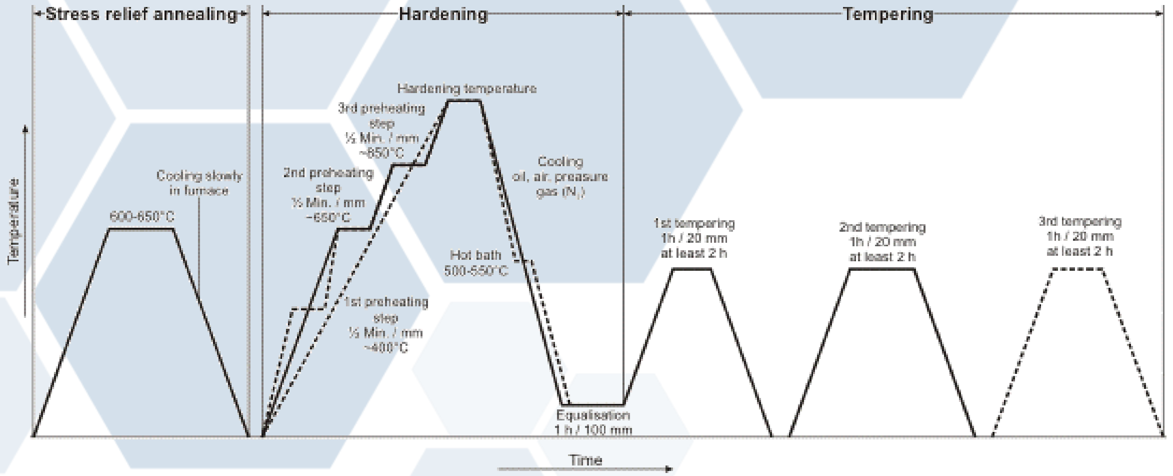

M.Kırbata, App.Mech. 2025, 6(1) 16

- **The cost of the steel and its heat treatment amounts can cover 25 % of the total cost of the die.**

Hardness - Fracture toughness – Wear resistance Relationship

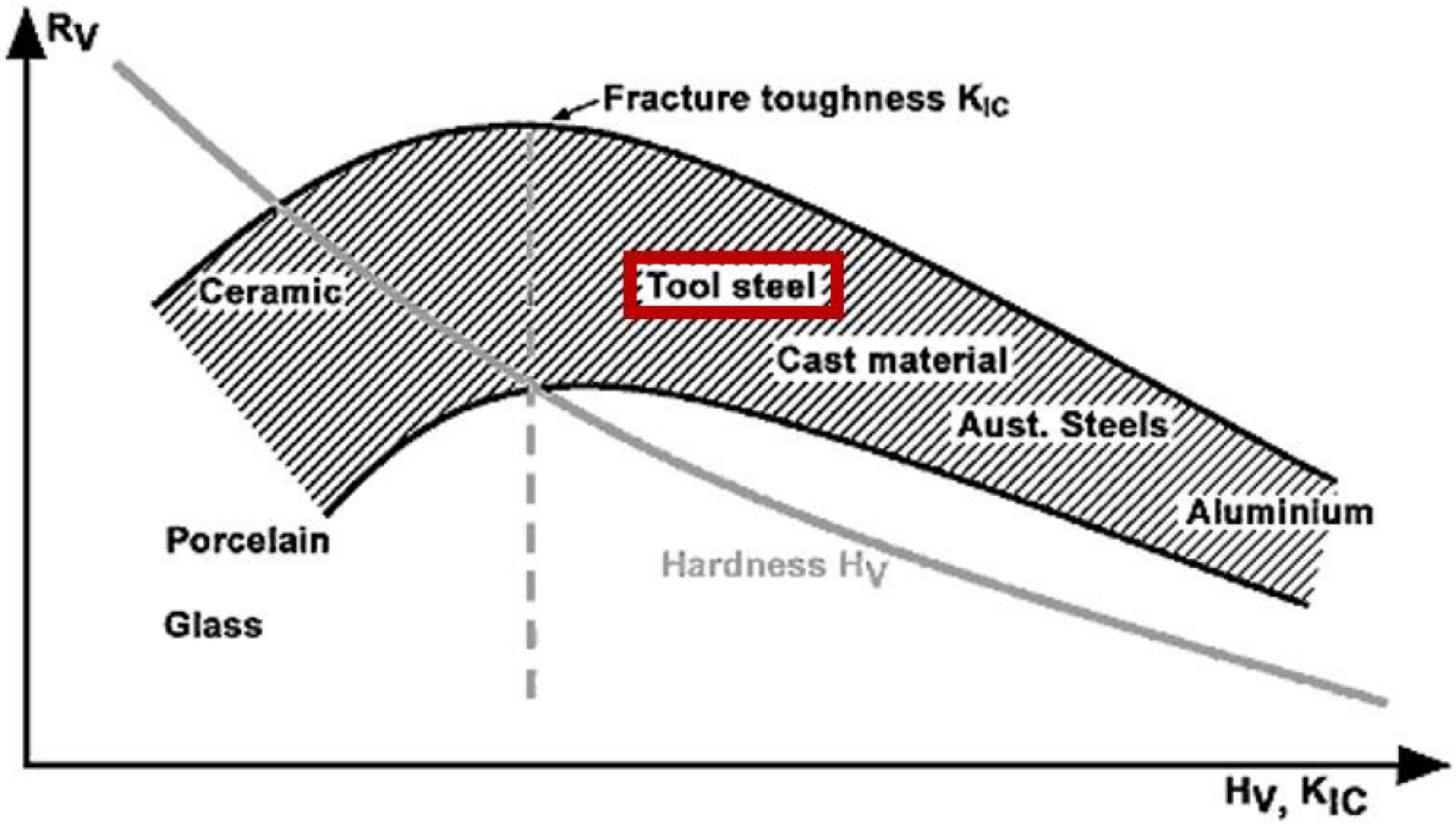

https://www.keramverband.de/brevier_engl/5/7/6/5_7_6_2.htm

Die Steels for Metal Forming Operations

Cold Work Die Steels

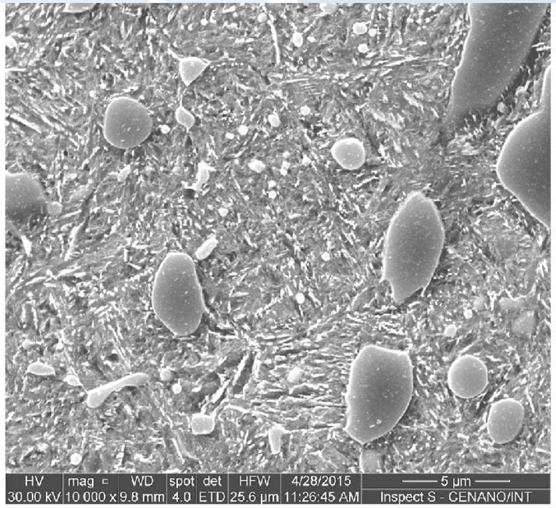

D2 / 1.2379 (X153CrMoV12)

- Main alloying elements: Cr (5%–12%), Mo, V (forming hard carbides)
- Target hardness: 58–64 HRC
- Microstructure: Tempered martensite matrix + uniformly distributed alloy carbides

Hot Work Die Steels

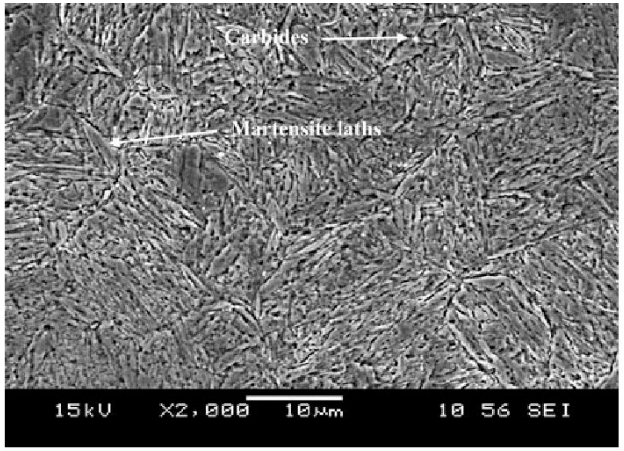

H13 / 1.2344 (X40CrMoV5-1

- Medium-to-low carbon content (0.3%–0.6%) to balance strength and toughness
- Main alloying elements: Cr (2%–5%), W, Mo, V (enhancing high-temperature strength)
- Target hardness: 58–64 HRC
- Microstructure: Tempered martensite/bainite + finely dispersed alloy carbides

Surface Modification

Nitriding	at 400–700 °C for 0.5–50 h	Increases hardness and plastic deformation resistance , improves the corrosion and oxidation resistance	Single and with some coating technology
Hybrid treatment	Thermochemical techniques with CVD or PVD coating	Increases wear resistant, and reduce the friction coefficient of alloy steel	Combination of thermochemical techniques with CVD or PVD
Pad welding	coats the tool with a metal layer during substrate melting	Improved life service (up to 60% in tool) ,quality and mechanical properties	With a coating technique
Beam technique	2.5 J/cm^2 energy required to melt and solidify the tool surface	Improves hardness up to 400HV in combination with another technique, makes thickness bigger than plasma nitriding	Single and combination
Mechanical treatment	surface is subjected to impacts from hard spheres moving at high velocity	Improves mechanical properties of surface, and generate residual stresses in metals	Single

A. Emamverdian , Y. Sun, C. Cao, .C. Prunc, Y. Wang, Engineering Failure Analysis 129 2021, 105678

Features of Nitrided Surfaces

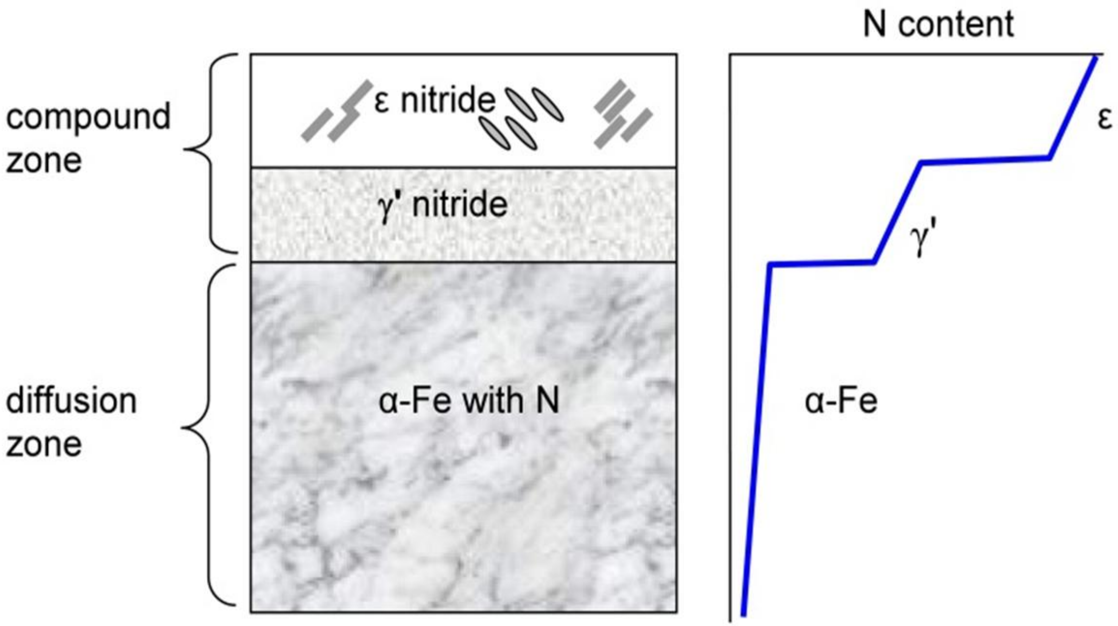

https://www.intechopen.com/chapters/39403

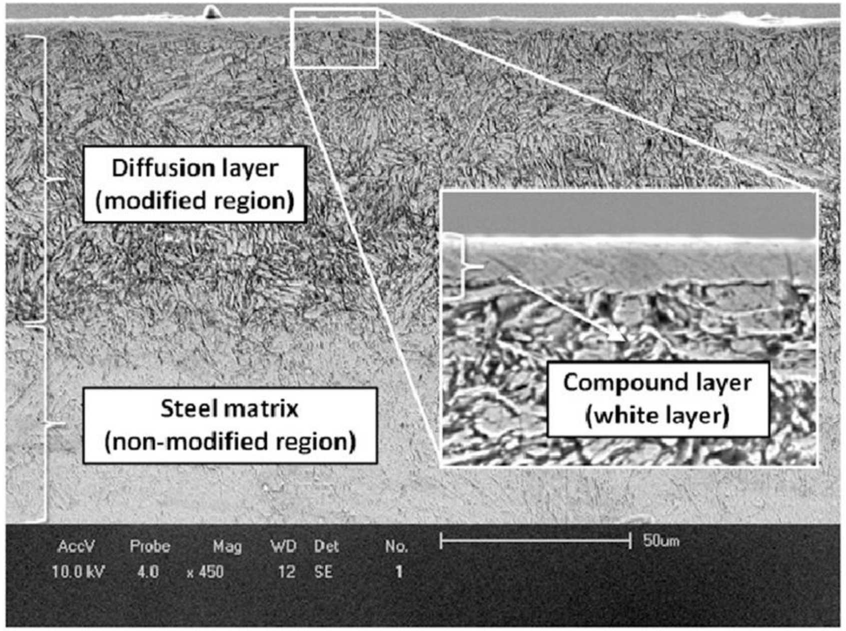

R. L.O. Basso, Corrosion Science, 52-9, 2010, 3133-3139

The compound layer consists primarily of iron nitrides, specifically epsilon (ϵ-$Fe_{2-3}N$) and gamma prim (γ'-Fe_4N) phases

The diffusion zone in a nitrided surface is the hardened region directly below the compound layer, where nitrogen dissolves into the lattice and forms alloy nitrides.

Properties of Nitrided Surfaces

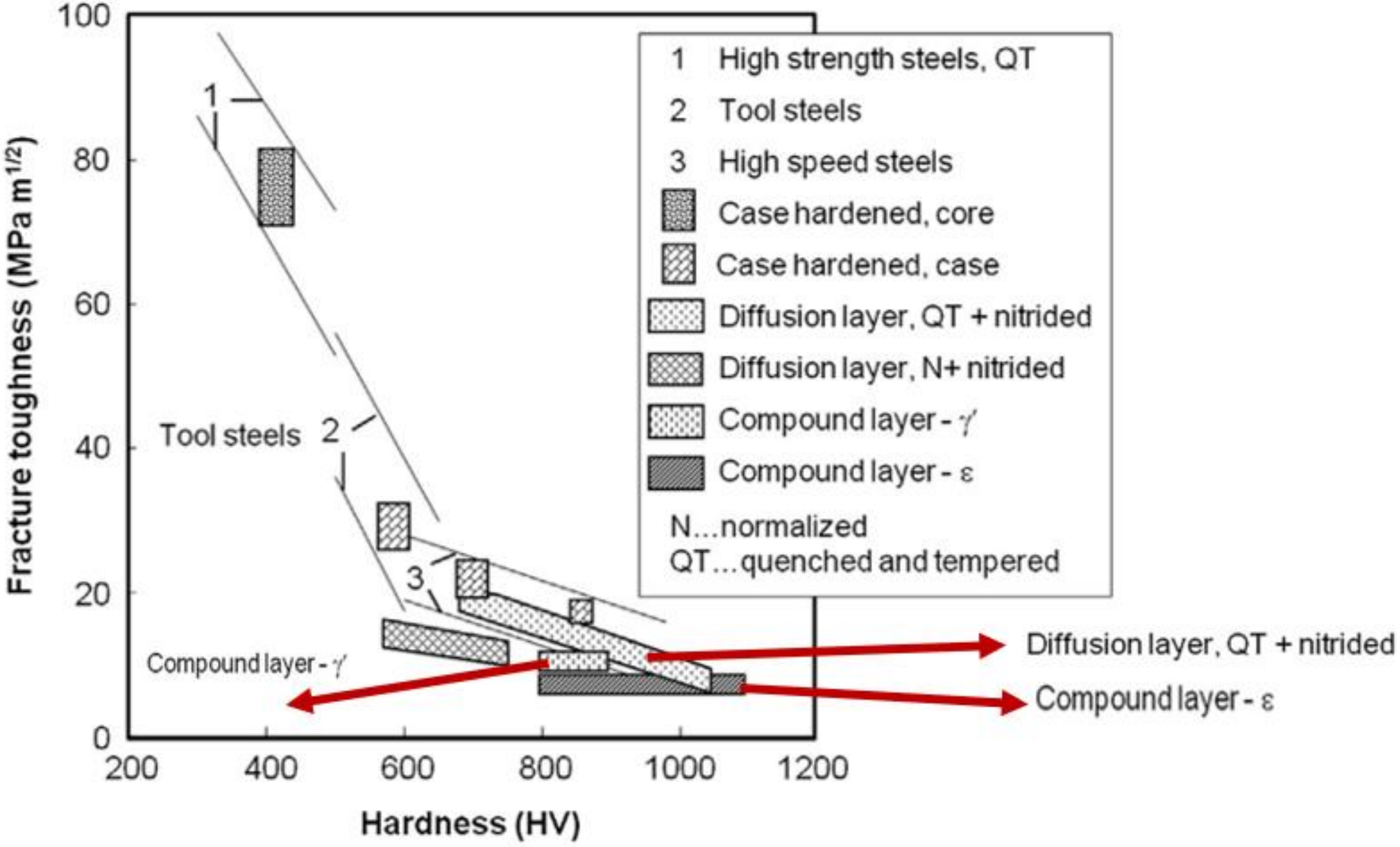

https://doi.org/10.1016/B978-0-08-096532-1.01216-4

Compound Layer Thickness vs Wear Resistance for Die Steels

Authors	Tool Steel Type/ Nitriding Process	Compound Layer Thickness	Counterface/Test Temperature	Concluding Remarks
B. Karamış [3,4]	Hot work (H13)/Plasma	5.5–16.8 µm	Nitrided H13 Steel/RT	Thick compound layer increases the wear rate
Fontalvo et al. [5]	Cold Work/Plasma	~2–15 µm	304 Steel/RT and 200 °C	Thinner compound layer is more efficient in reducing wear while thicker layer may easily spall
Terčelj et al. [6]	Hot work (H13)/Plasma and Gas	0–18 µm	6063 Al alloy/510 °C	High thickness of the compound layer leads to earlier spalling
Castro et al. [7]	Hot work (H13)/Salt Bath	0–24 µm	Al_2O_3/500 °C	Thinner compound layer is effective for shorter sliding distance, Thicker and harder NDZ is beneficial for longer sliding distance
Karamış et al. [8]	Hot work (H11)/Plasma	4–5 µm	52100 Steel/RT	Similar wear performance is obtained from 4 to 5 µm thick compound layers
Mohammadzadeh et al. [9]	High speed (M2)/ Plasma	Not given	Al_2O_3/RT	Lower wear rate is obtained by avoiding compound layer formation
Das et al. [10]	Hot work (H13)/Plasma	4–11 µm	Al_2O_3/RT	Thinner compound layer exhibits better wear resistance
Wang et al. [11]	Hot work (H13)/Gas	max. ~10 µm	52100 Steel/RT	Increase in the testing load results in higher wear rate for the thick compound layer Compound layer free surfaces and thin compound layer show better wear resistance at the highest testing load
Kumar et al. [12]	Hot work (H13)/Plasma	14–87 µm	5120 Steel/RT - 600 °C	Thinner compound layer has a positive effect on wear resistance
Diaz-Guillen et al. [13]	Cold Work (D2)/Plasma	0–8 µm	WC/RT	Presence of the compound layer caused severe wear by removal of hard particle from the surface

Compound layers having thickness << 5 μm exhibit higher wear resistance under sliding contact

Kaba et al., Wear ,498–499, 15 June 2022, 204300

Case 1

Wear of forging-extrusion dies used in manufacturing of engine valves

Wear 498-499 (2022) 204300

Contents lists available at ScienceDirect

Wear

journal homepage: www.elsevier.com/locate/wear

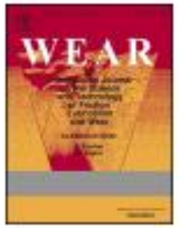

Surface degradation of nitrided hot work tool steels under repeated impact-sliding contacts: Effect of compound layer

M. Kaba [a], M. Altay [a], E. Akyildiz [a], F. Muhaffel [a], S. Ozkurt [b], E. Atar [c], M. Baydogan [a], H. Cimenoglu [a,*]

[a] *Department of Metallurgy and Materials Engineering, Istanbul Technical University, Istanbul, Turkey*
[b] *Supsan Motor Supaplari San. Tic. A. S, Istanbul, Turkey*
[c] *Department of Materials Science and Engineering, Gebze Technical University, Kocaeli, Turkey*

ARTICLE INFO

Keywords:
Nitriding
Compound layer
Hot work tool steel
Wear mechanism
Impact-sliding wear

ABSTRACT

Wear behaviour of quenched and tempered (QT) hot work tool steels (Uddeholm QRO90) was investigated against SAE 52100 grade bearing steel balls after gas nitriding using a dedicated laboratory scale impact-sliding wear test rig. Gas nitriding was employed in a fluidised bed reactor under two alternative regimes: i. "High Temperature Nitriding (HTN)" carried out at 510 °C and ii. "Low Temperature Nitriding (LTN)" carried out at ≤ 400 °C. The HTN process resulted in the formation of ~2 μm thick external compound layer, whereas the LTN processed steels were free of any surface compound layer formation. After the impact-sliding wear tests employed at room temperature (RT), the prevailing wear mechanisms of the examined steels were assessed as tribo-oxidation and fatigue wear. The testing at 600 °C induced different wear mechanisms for the HTN and the LTN steels. While tribo-oxidation and fatigue wear were preserved for the HTN steel, plastic deformation dominated the wear that progressed on the compound layer free surface of the LTN steel. Impact-sliding wear testing at 600 °C showed that the wear rate of LTN > HTN steels, as opposed to the wear rate at RT where wear rate of HTN > LTN.

Production of Engine Valves

Engine valves are mechanical components in internal combustion engines that regulate the intake of air-fuel mixtures and the exhaust of combustion gases.

https://engineprofessional.com/articles/EPQ322_66-78.pdf

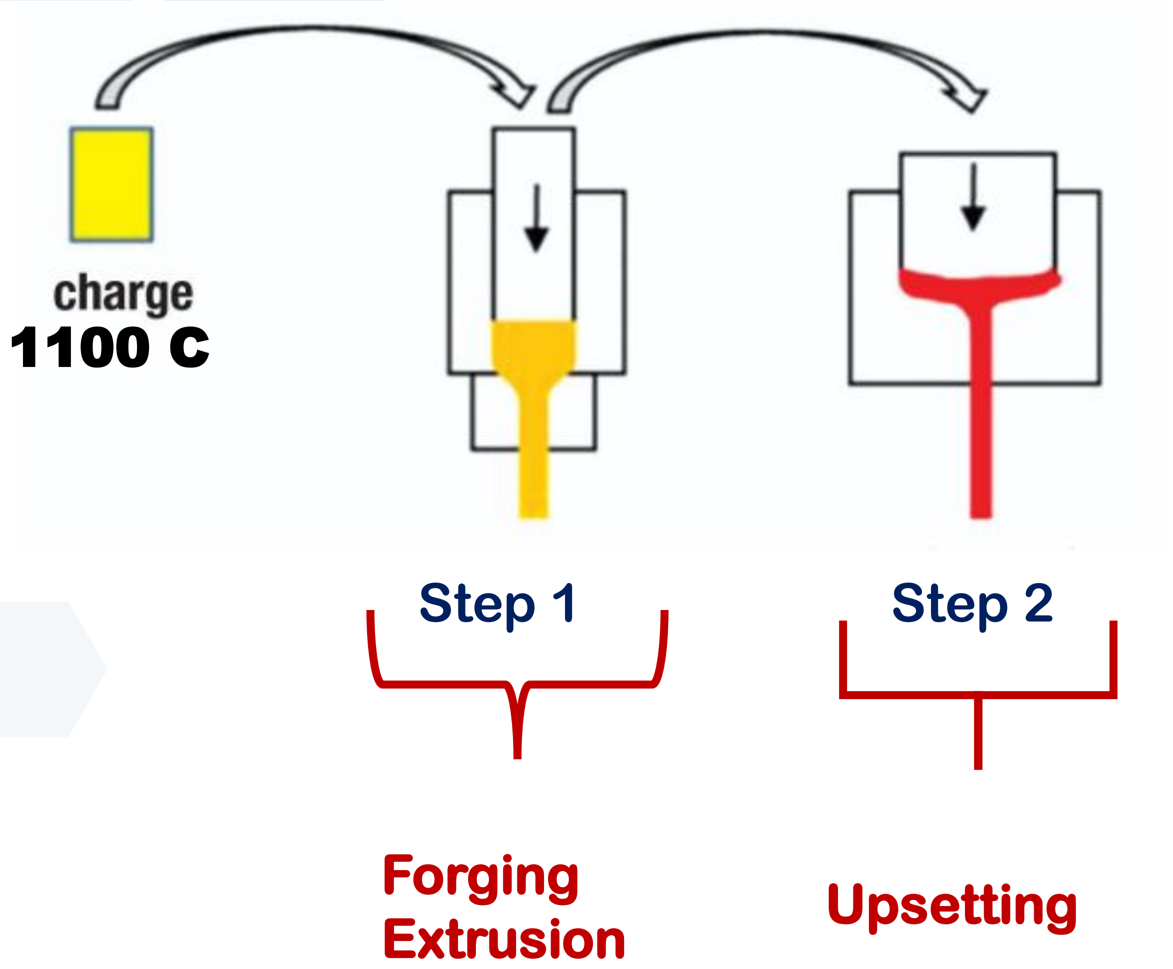

Problem: Interuption of mass production in every 1h due to replacement of worn dies with the new ones

Worn Surface Examination on the Nitrided Forging - Extrusion Die failed after ~ 500 operations

Die Material :

Hot work tool steel
0.38C-2.6Cr-2.3Mo-0.9V
(Uddeholm QRO90)

Heat Treatment:

Q&T (580 HV) + Gas Nitriding

Valve Material:

0.45C-9Cr-3Si steel

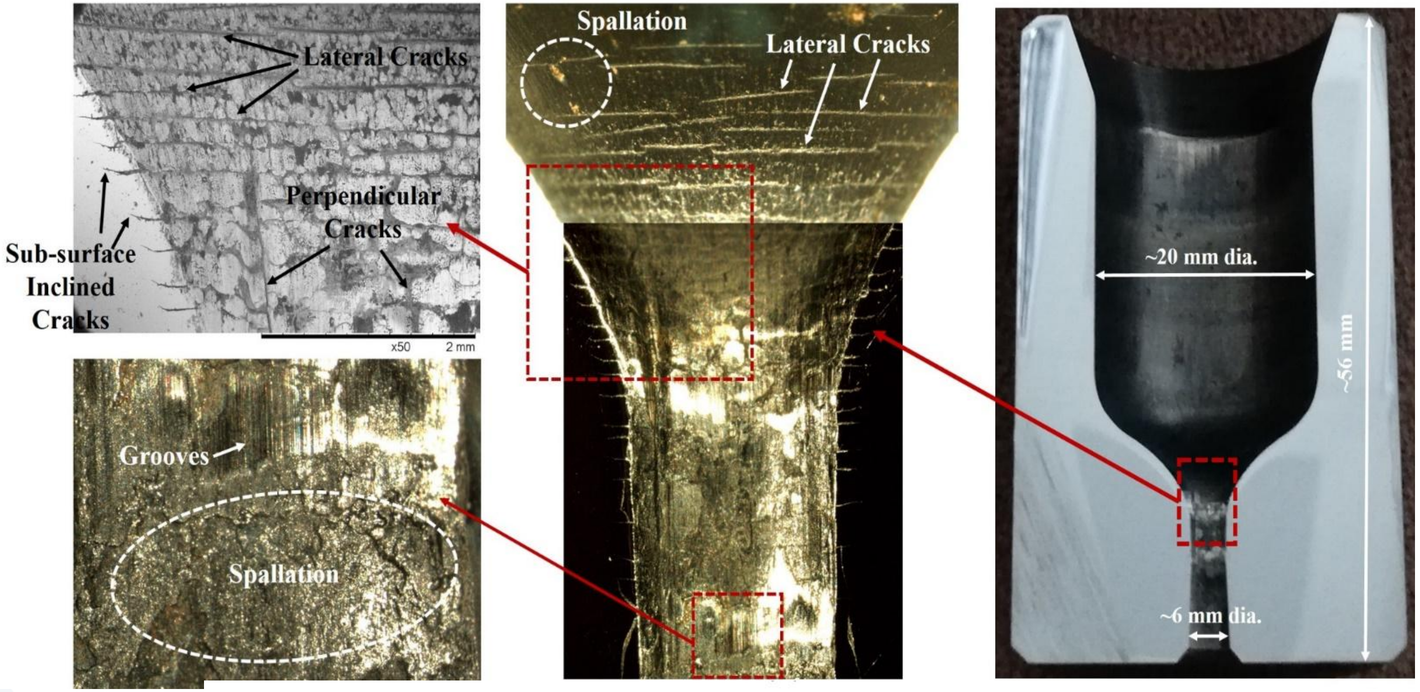

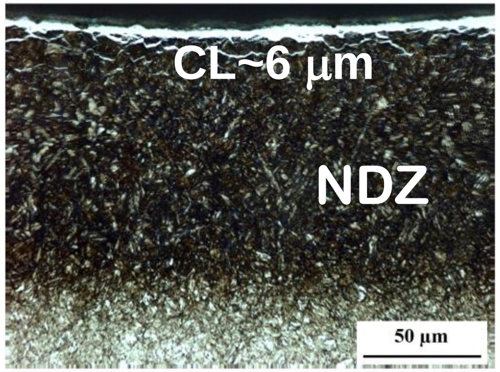

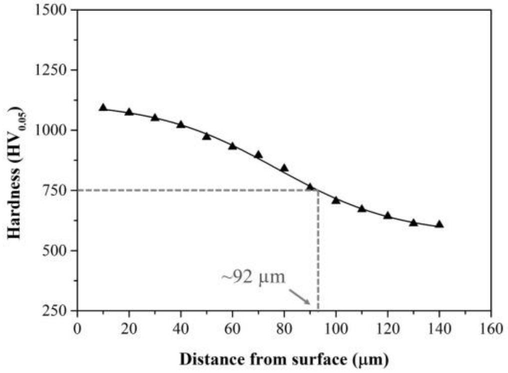

Experimental Work: Gas Nitriding Process

The nitriding atmosphere was a mixture of 60% NH_3 and 40% N_2.

HTN

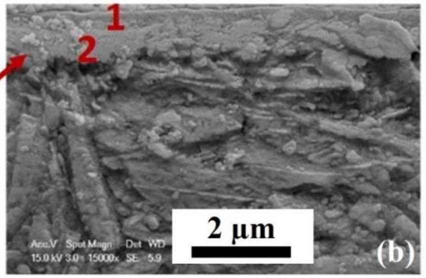

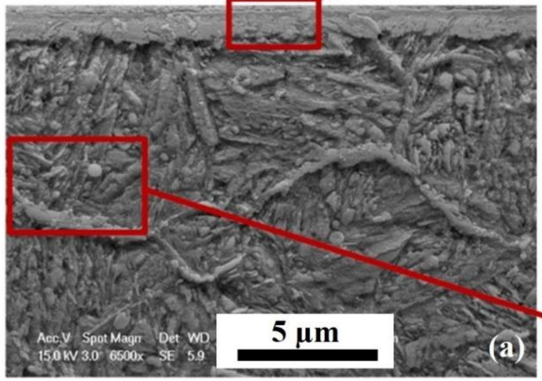

at. %	1	2	3	4
Fe	56.36	75.08	59.15	74.31
N	29.74	14.32	20.97	14.45
Cr	4.69	2.82	2.49	2.31
Mo	7.91	7.13	9.29	8.25
V	1.30	0.65	8.10	0.67

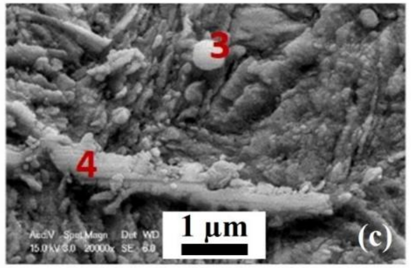

510 °C for 6 h

~2µm thick CL - 1644 $HV_{0.05}$

LTN

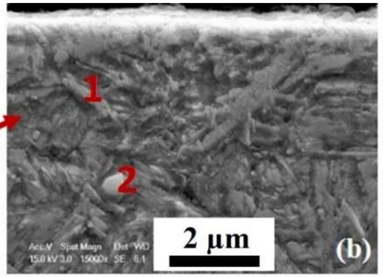

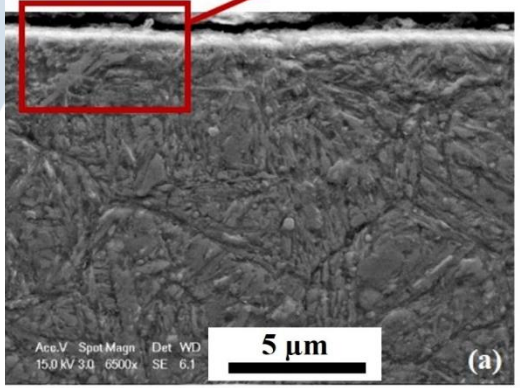

at. %	1	2
Fe	56.43	72.56
N	38.10	17.60
Cr	1.44	2.16
Mo	3.24	3.82
V	0.79	3.86

400 °C for 6 h
+
375 °C for 6h

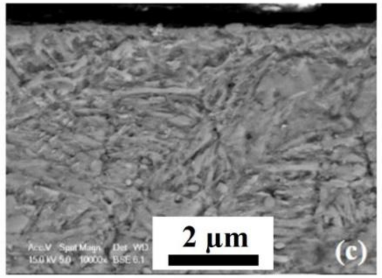

No CL - 1593 $HV_{0.05}$

Case Depth

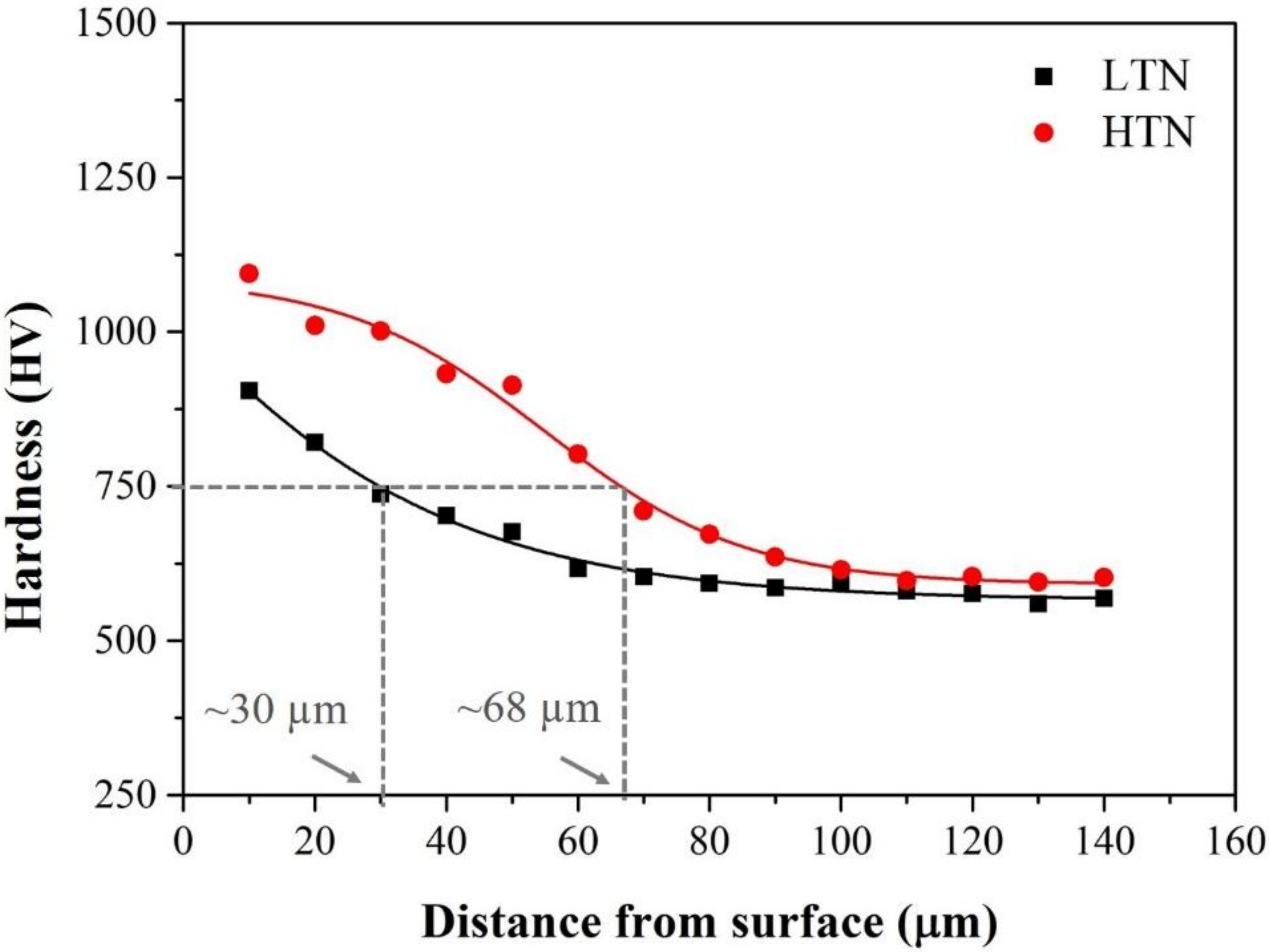
1500
1250
1000
750
500
250
Hardness (HV)
0
20
40
60
80
100
120
140
160
Distance from surface (µm)
LTN
HTN
~30 µm
~68 µm

Phase Analysis

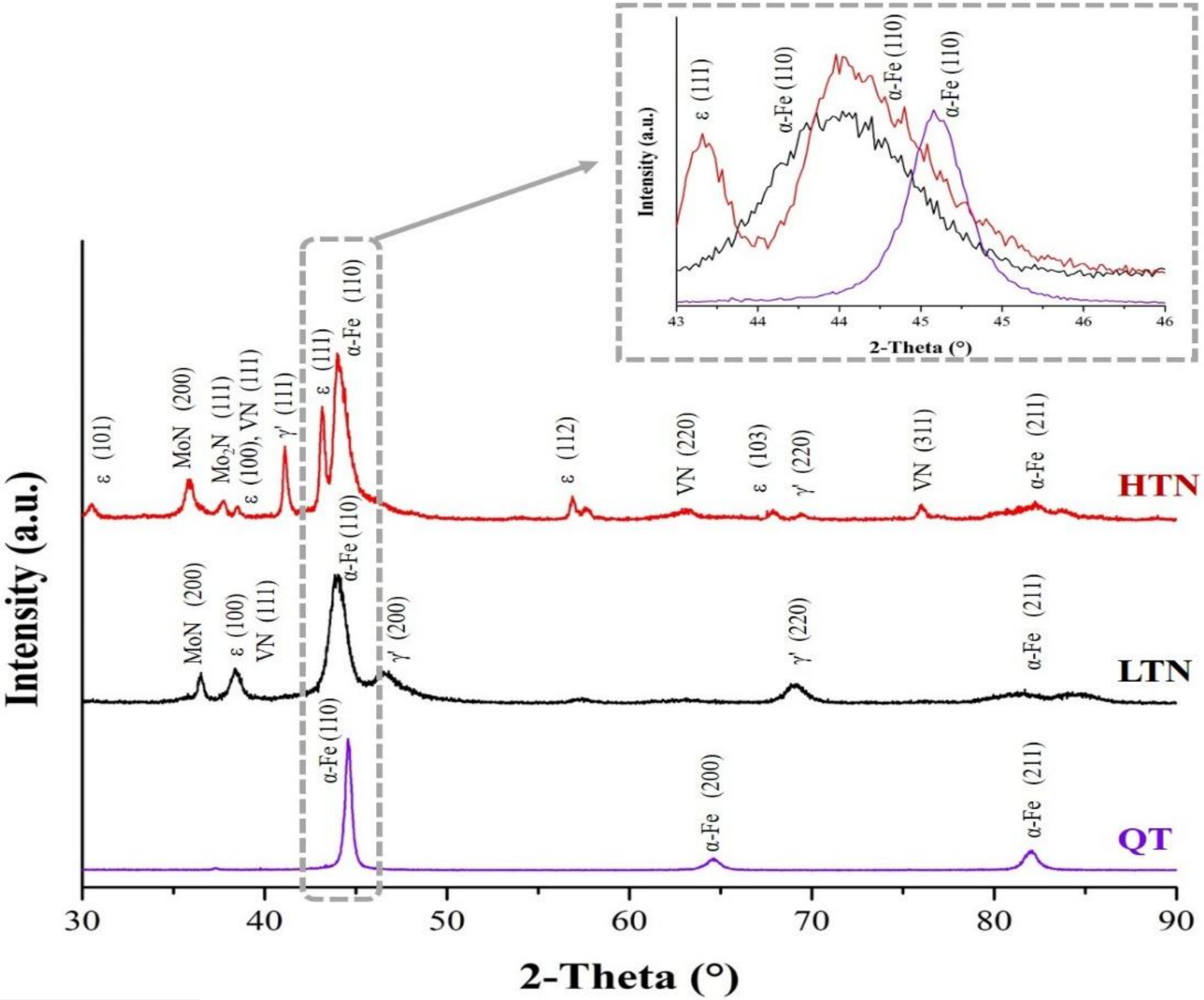

From the α′-Fe (110) peaks;

Elastic distortion of the lattice imposing compressive residual stress within NDZ calculated as:

1.3% for HTN steel and

1.6% for LTN steel

Forging – Extrusion Step of Valve Production

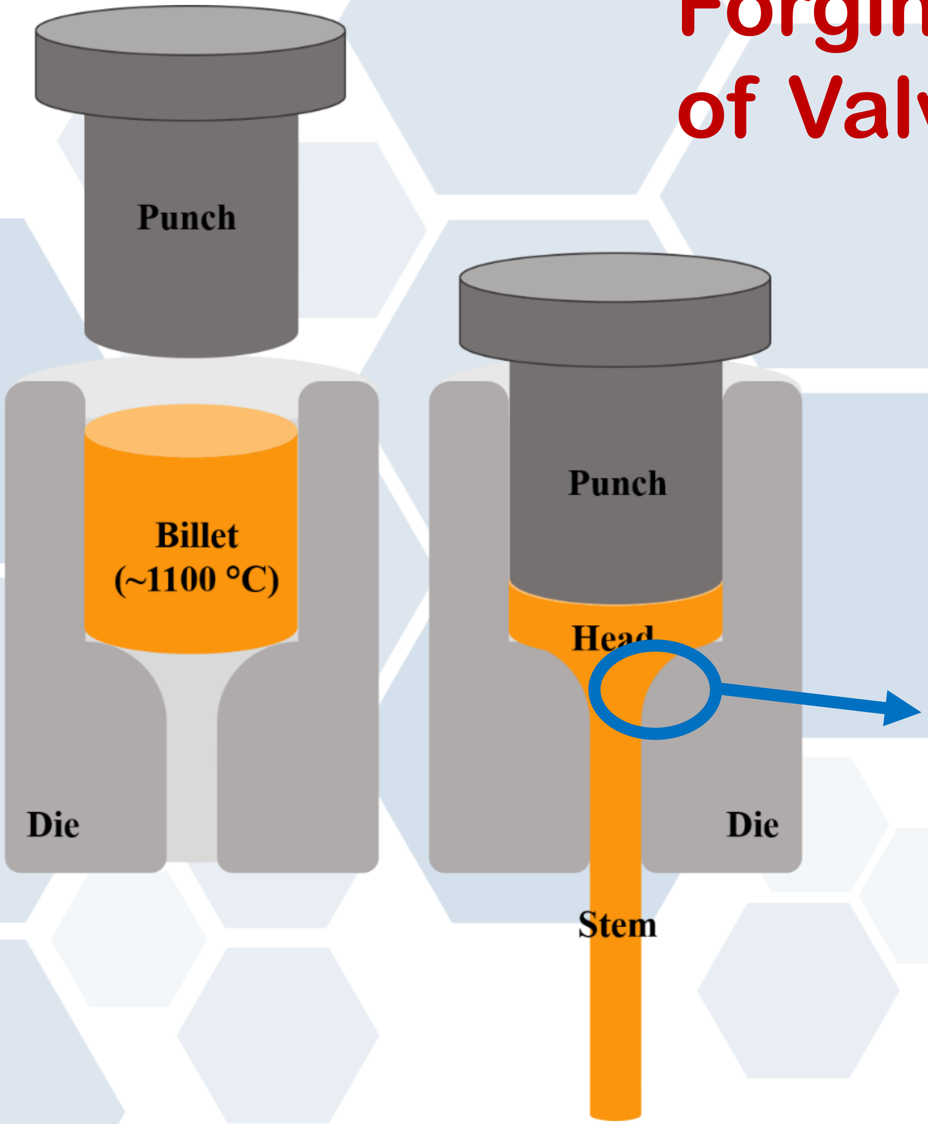

Impact- Sliding Contact

Impact - Sliding Wear Tester

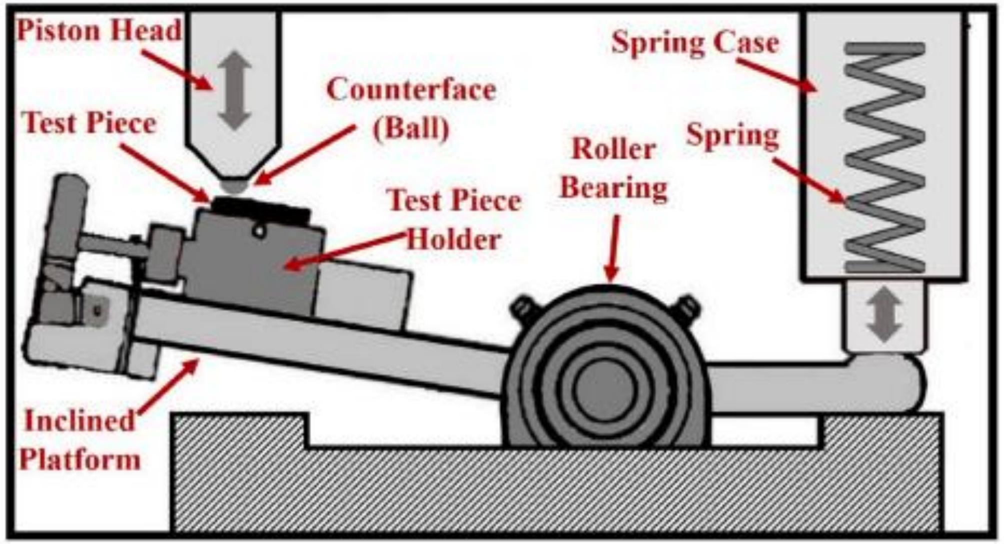

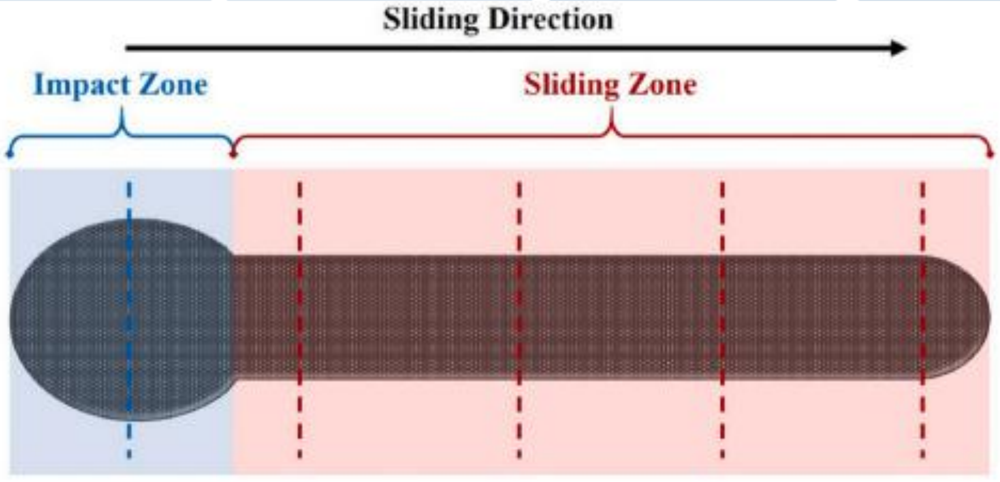

DOI: 10.1016/j.wear.2022.204300

US008402811B2

(12) **United States Patent**
Nie et al.

(10) **Patent No.:** **US 8,402,811 B2**
(45) **Date of Patent:** **Mar. 26, 2013**

(54) **CYCLIC IMPACT-SLIDING FATIGUE WEAR TESTING INSTRUMENT**

(76) Inventors: **Yining Nie**, Windsor (CA); **Jingzeng Zhang**, Windsor (CA)

(*) Notice: Subject to any disclaimer, the term of this patent is extended or adjusted under 35 U.S.C. 154(b) by 365 days.

(21) Appl. No.: **12/824,172**

(22) Filed: **Jun. 26, 2010**

(65) **Prior Publication Data**

US 2011/0314894 A1 Dec. 29, 2011

(51) **Int. Cl.**
G01M 7/00 (2006.01)

(52) **U.S. Cl.** **73/12.09**

(58) **Field of Classification Search** 73/12.09
See application file for complete search history.

(56) **References Cited**

FOREIGN PATENT DOCUMENTS

EP 1320681 * 6/1987

* cited by examiner

Primary Examiner — Lisa Caputo
Assistant Examiner — Octavia Davis-Hollington

(57) **ABSTRACT**

This invention deals with a testing instrument that is used to investigate failure behavior of items subject to impact and sliding forces. The testing instrument produces an impact motion and a sliding motion in each testing cycle with maximum contact pressure similar to actual stresses applied to the items during real applications. The invented instrument simulates wear conditions and failure behaviors of biomedical implants, components, tools and coatings which are observed in practical applications.

17 Claims, 3 Drawing Sheets

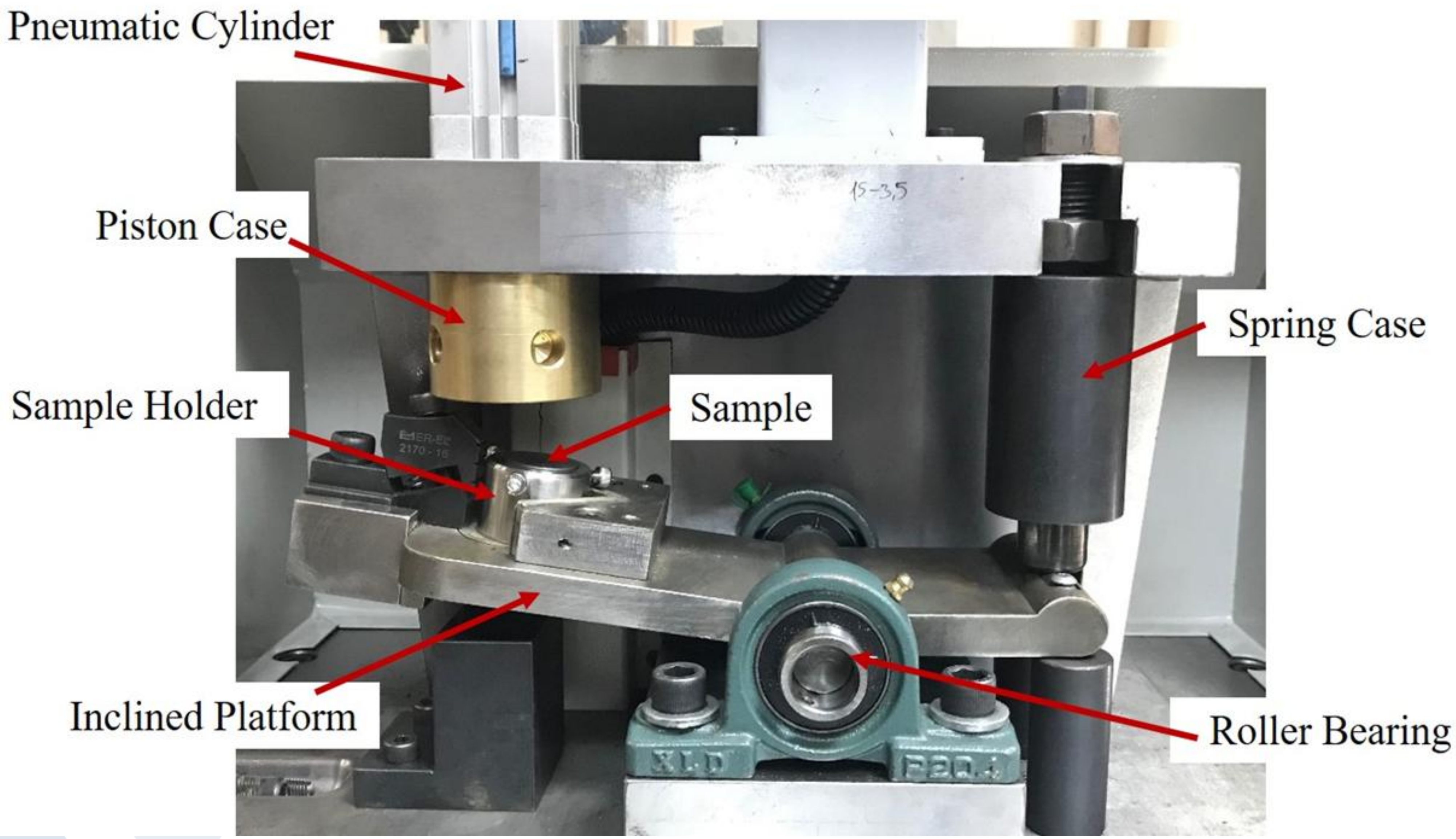
Pneumatic Cylinder
Piston Case
Spring Case
Sample Holder
Sample
Inclined Platform
Roller Bearing

Impact Sliding Wear Testing Parameters

The maximum loads: 35 N (impact) and 150 N (sliding)

Loading cycles: 1000

Test duration: 4 min

Counterface: 10 mm dia 52100 grade bearing steel ball (~850 HV).

Test temperature: RT and 600C

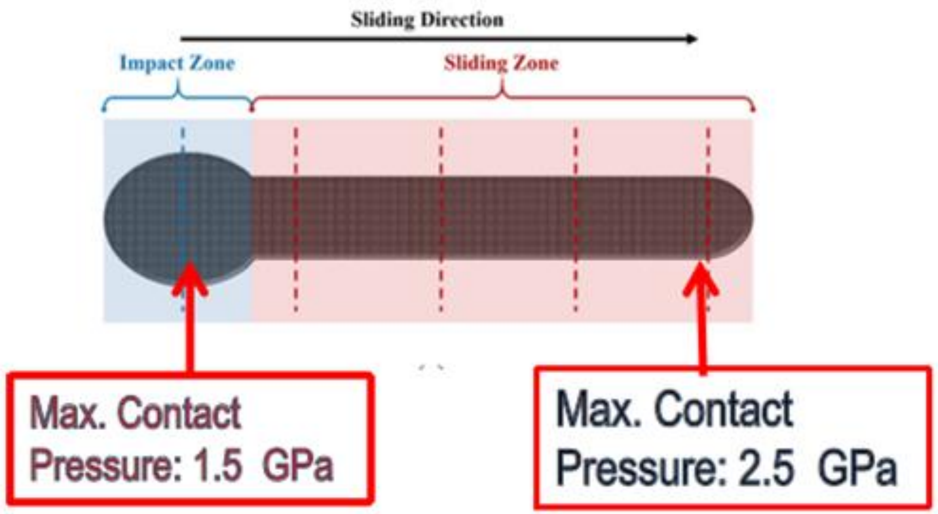

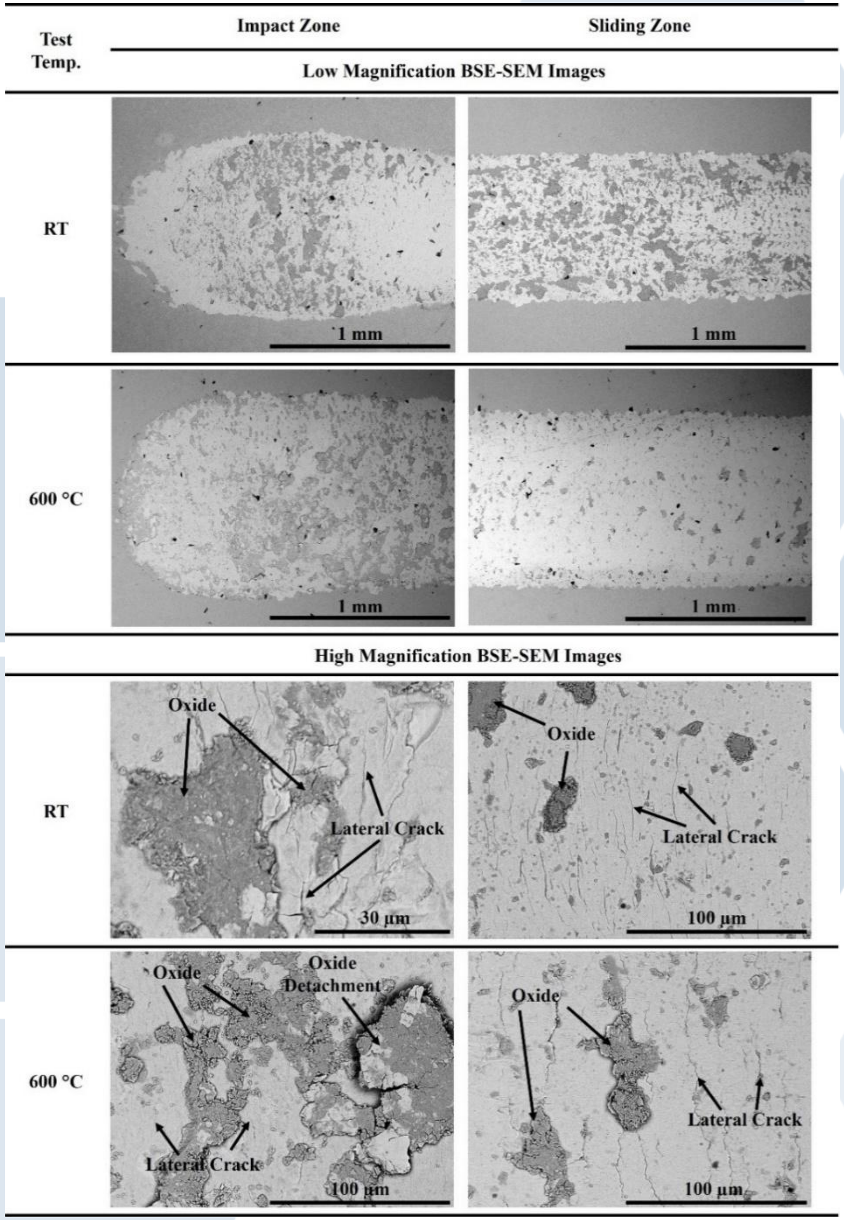

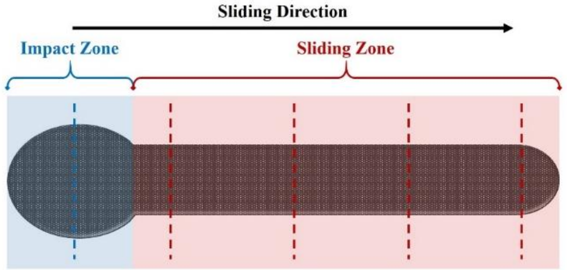

Wear Track Examinations on HTN Steel

Wear Mechanism
RT & 600 °C

Tribo-oxidation
+
Fatigue Wear

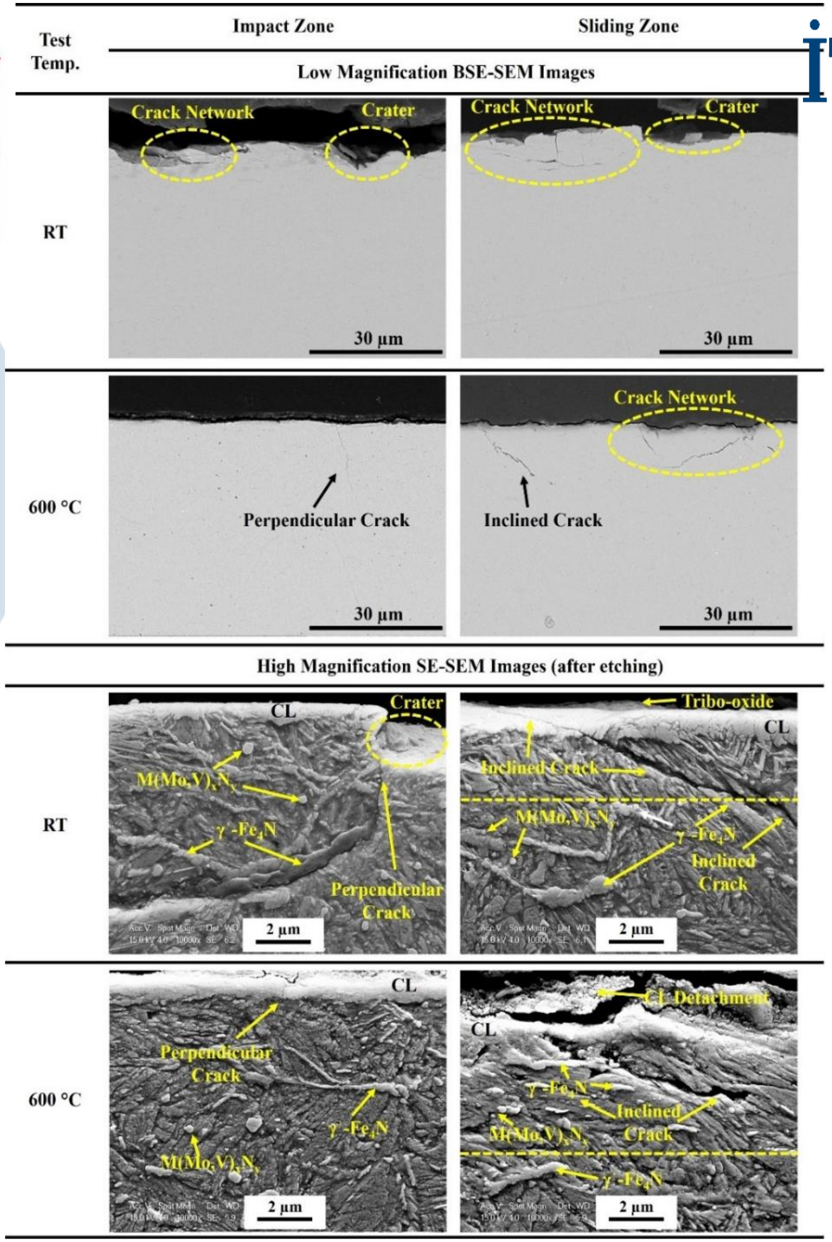

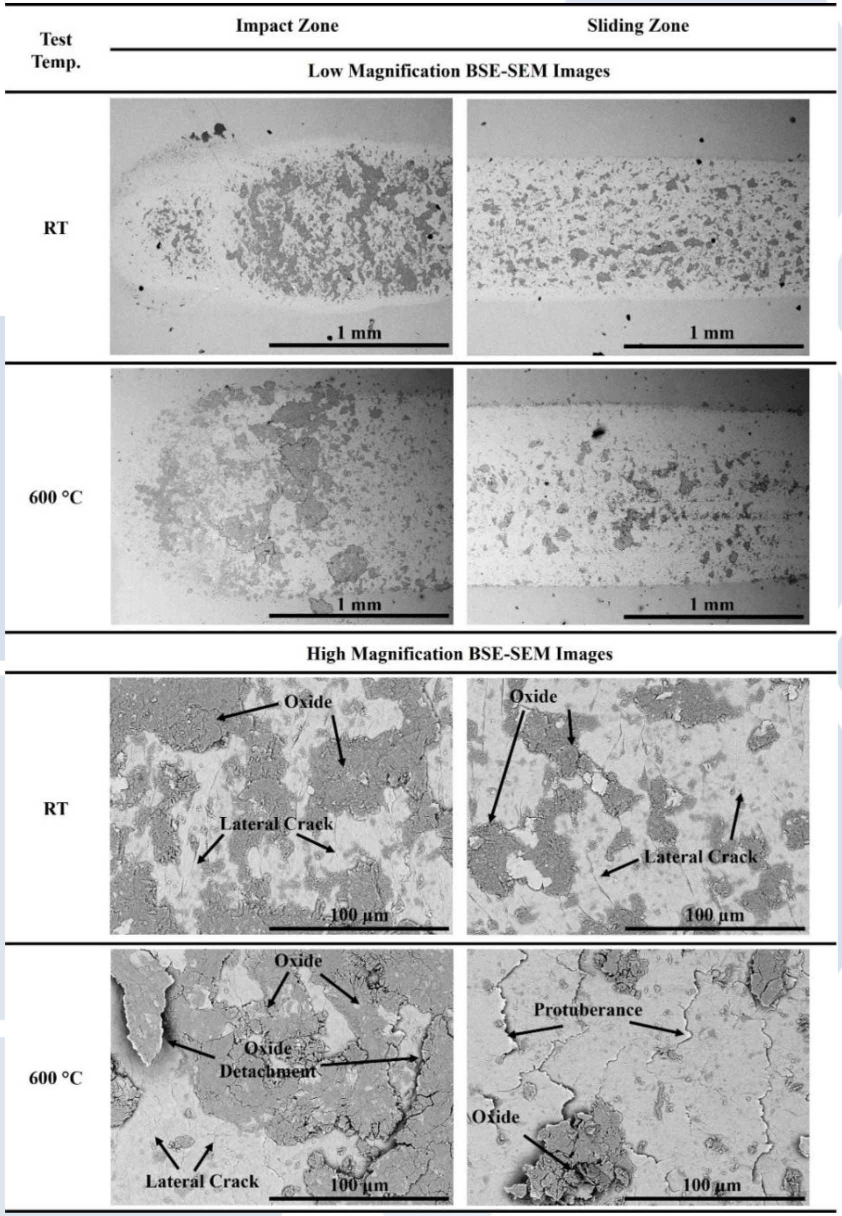

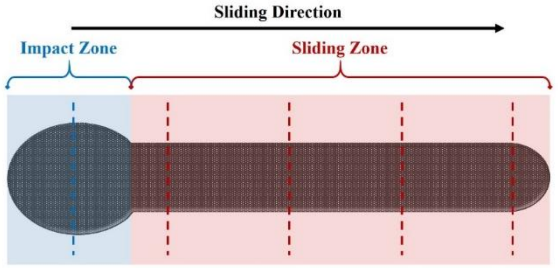

Wear Track Examinations on LTN Steel

<u>Wear Mechanism</u>

RT

Tribo-oxidation

+

Fatigue Wear

600 °C

Plastic Deformation

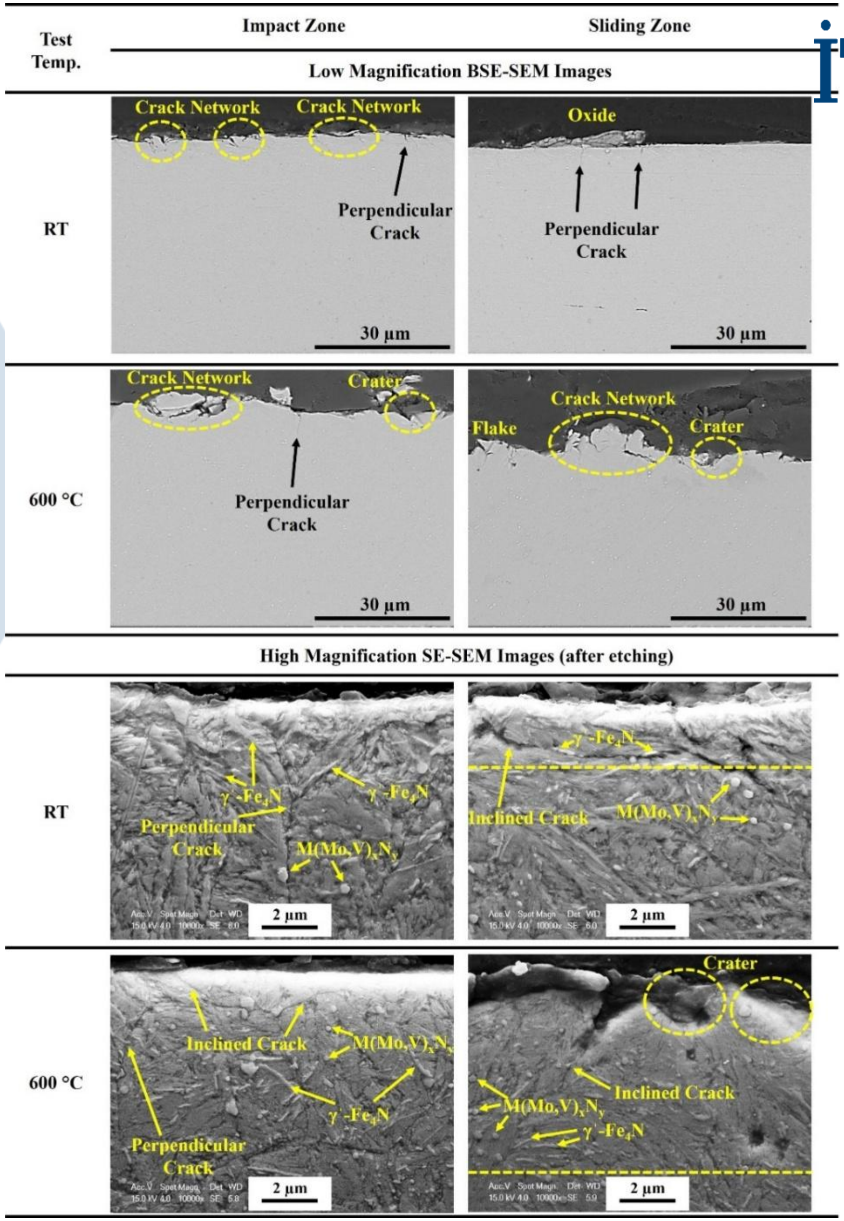

Wear Loss of the HTN and LTN Steels

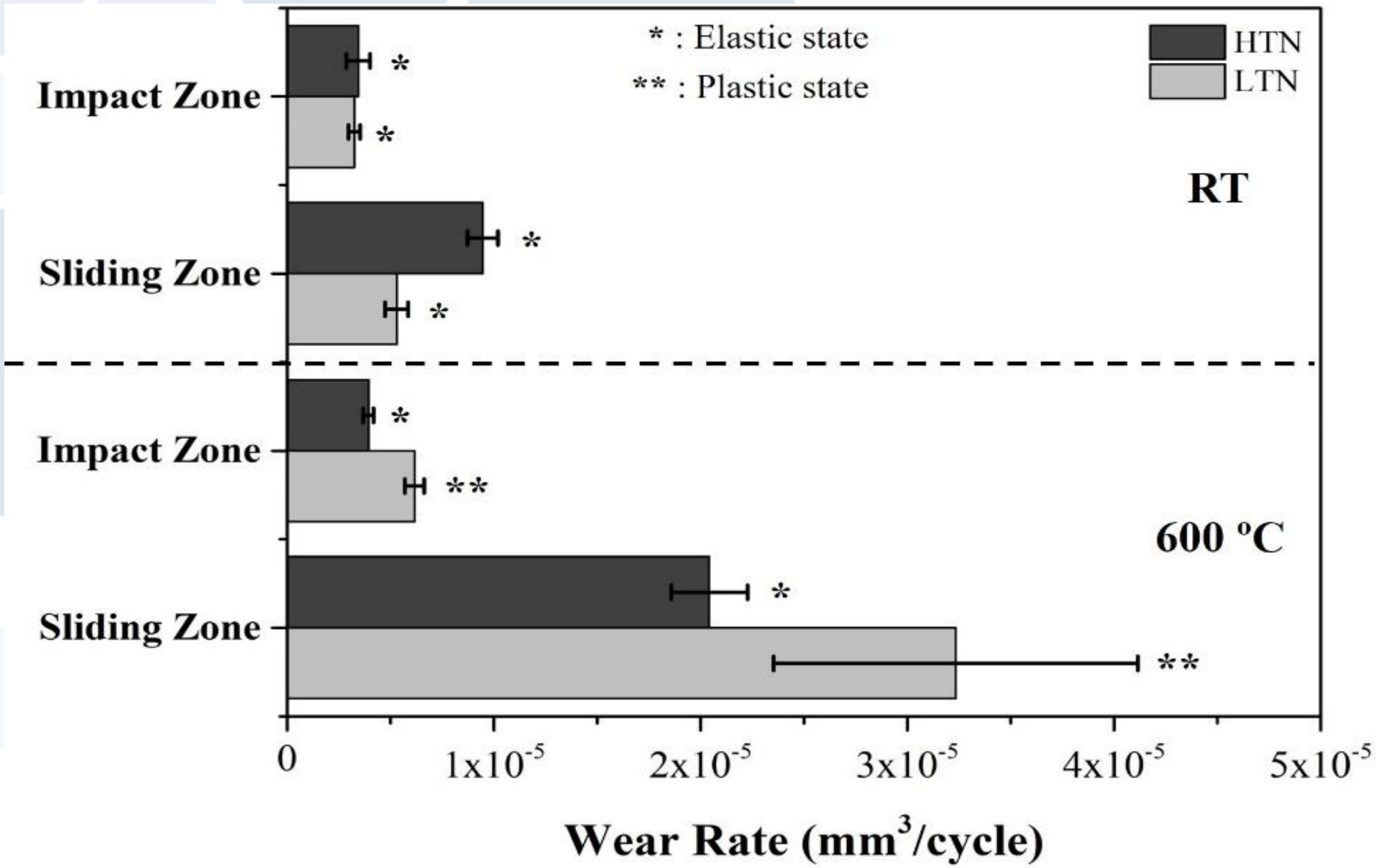

Progress of Wear on HTN and LTN Steels at RT

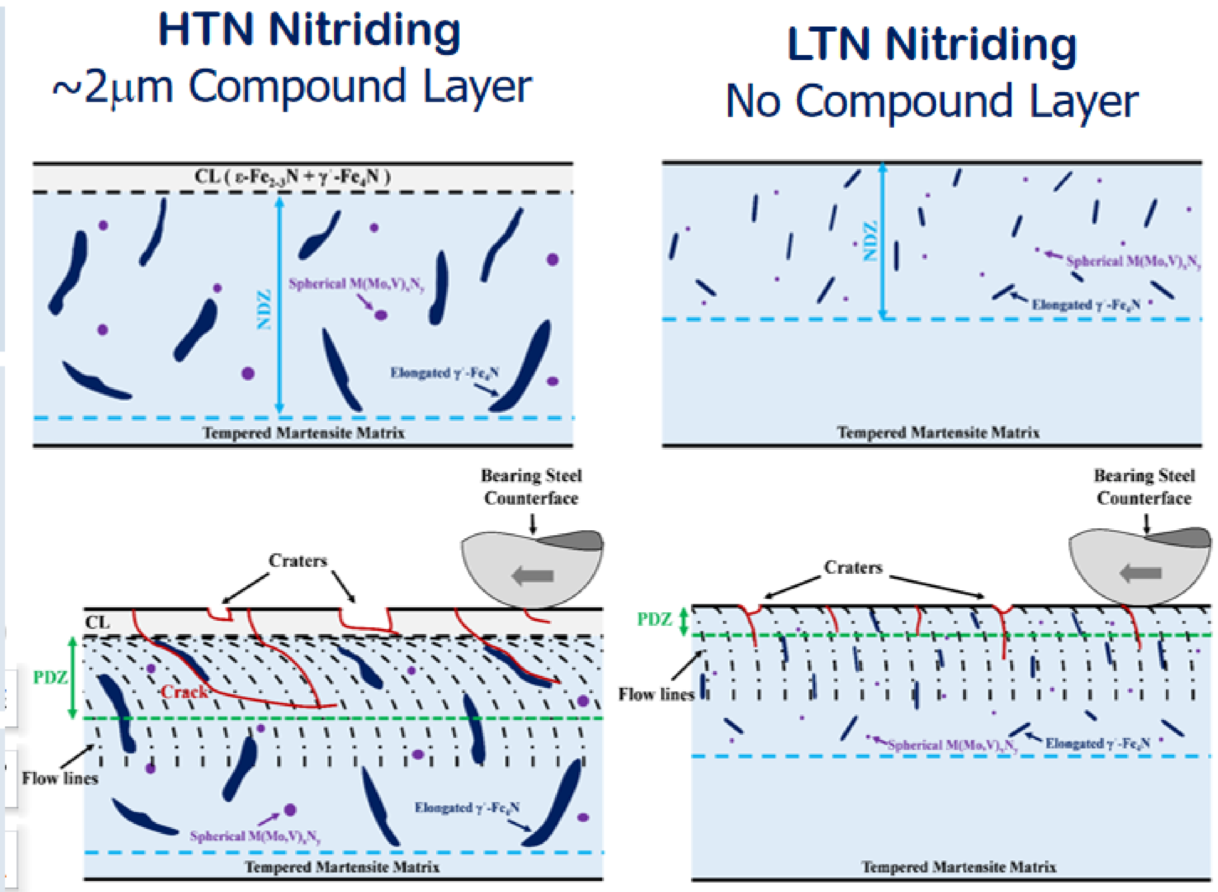

At 600 C

- Similar wear mechanism was operative for the HTM steel
- LTN steels severely worn via plastic deformation

Field Tests of Forging -Extrusion Dies

(Thin Compound Layer Covered)

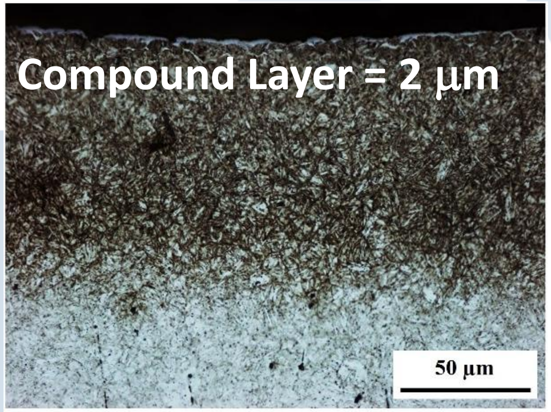

Gas Nitrided under K_N Controlled Mode

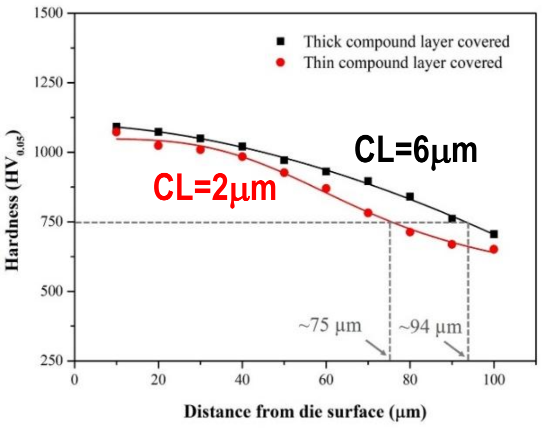

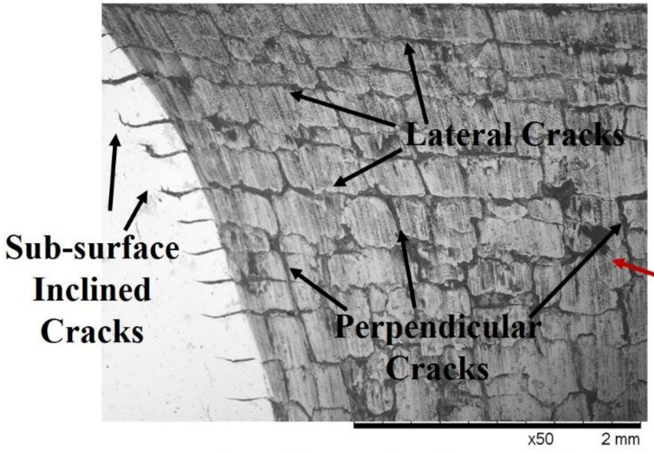

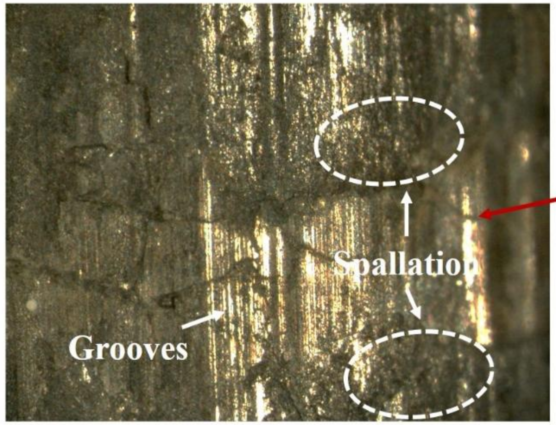

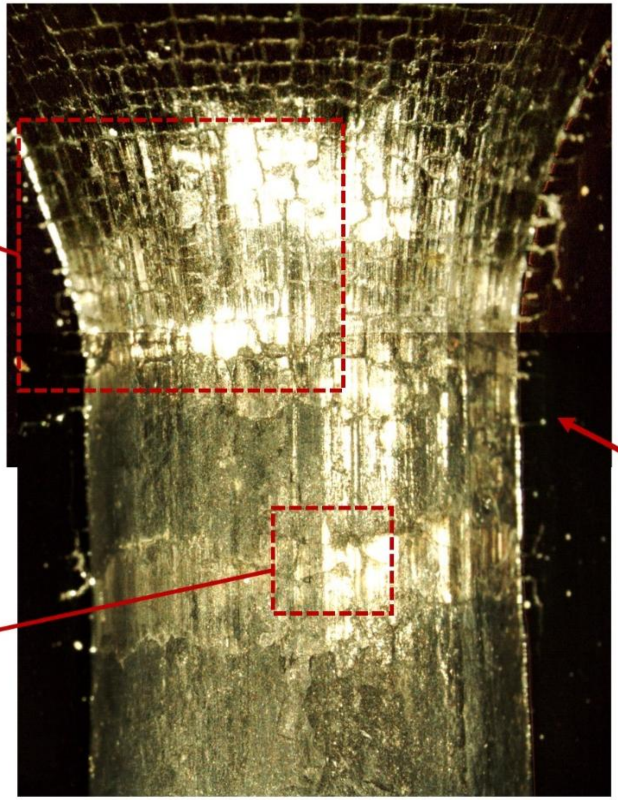

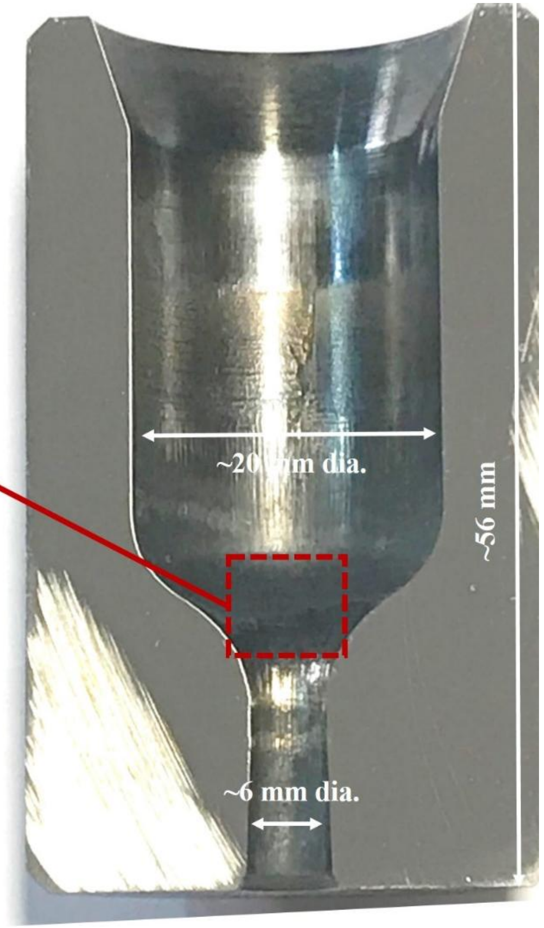

Failed after ~800 operations
Service life increased 60 %

Case 2

Effect of Microstrure on the Performance of Trimming Dies Manuractured from Cold Work Die Steel

Previous Work

Wear 426–427 (2019) 1635–1645

Contents lists available at ScienceDirect

Wear

journal homepage: www.elsevier.com/locate/wear

ELSEVIER

Mechanisms of die wear and wear-induced damage at the trimmed edge of high strength steel sheets

Check for updates

Z. Cui, S. Bhattacharya, D.E. Green, A.T. Alpas*

Department of Mechanical, Automotive and Materials Engineering, University of Windsor, 401 Sunset Avenue, Windsor, ON, Canada N9B 3P4

A R T I C L E I N F O

Keywords:
Die wear
Trimming
DP980 steel
D2 tool steel
Shear affected zone
Subsurface strains

A B S T R A C T

Die wear during trimming of advanced high strength steel (AHSS) sheets deteriorates the edge quality of trimmed sheets. In this work, the mechanisms of AISI D2 steel trim die wear and their effects on plastic deformation and fracture behaviour of the sheared edge of DP980 steel sheet were examined. A mechanical press equipped with D2 inserts was used to trim DP980 sheets with a clearance of 0.14 mm (10%). Abrasion and microchipping were identified as the wear mechanisms operating at the upper die, with microchipping becoming more dominant after 60,000 trimming cycles. The burr height and the length of the burnish zone of sheared DP980 sheets increased linearly with the chipped die edge percentage. The shear strains in the shear effected zone (SAZ) were estimated using martensite displacements as metallographic markers in the ferrite matrix as a function of the depth beneath the sheared edge. The depth of SAZ, and the plastic strains at a given depth within the SAZ increased with the number of trimming cycles. Correlation of the local stress and strain values generated in the SAZ showed that a saturation flow stress was reached near the sheared edge. The damage in SAZ occurred in the form of crack formation at the martensite/ferrite interfaces and fracture of martensite. Die wear reduced the tensile ductility of the DP980 sheets, and the fracture mode in tension changed from ductile with localized neck to more brittle sheared edge fracture initiating from surface cracks after 60,000 cycles.

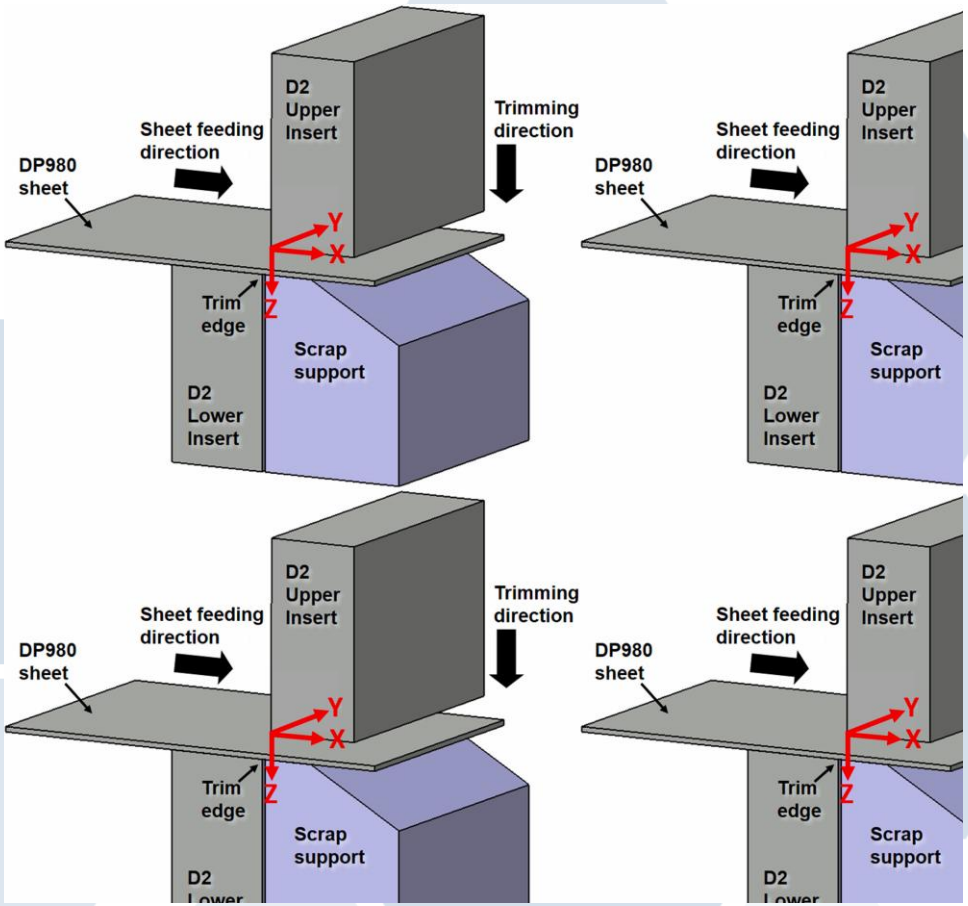

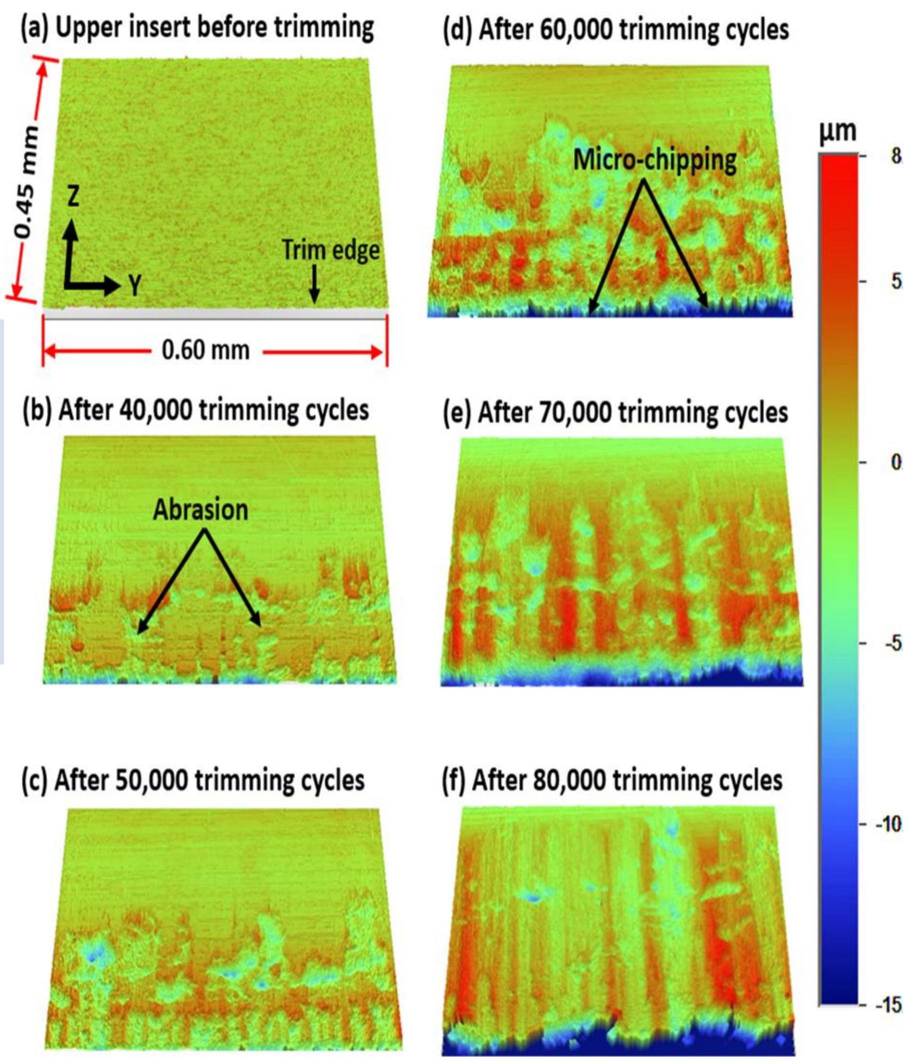

DP 980 Steel

Microstructure: 70% M + 30% F
Yield Strength: 775 MPa
Tensile strength: 999 MPa.
Total elongation: 14.1%
Thickness of 1.4 mm

3-dimensional optical profilometer images of the trim edges obtained from the YZ-plane of the upper insert (a) before trimming and after (b) 40,000, (c) 50,000, (d) 60,000, (e) 70,000, and (f) 80,000 trimming cycles.

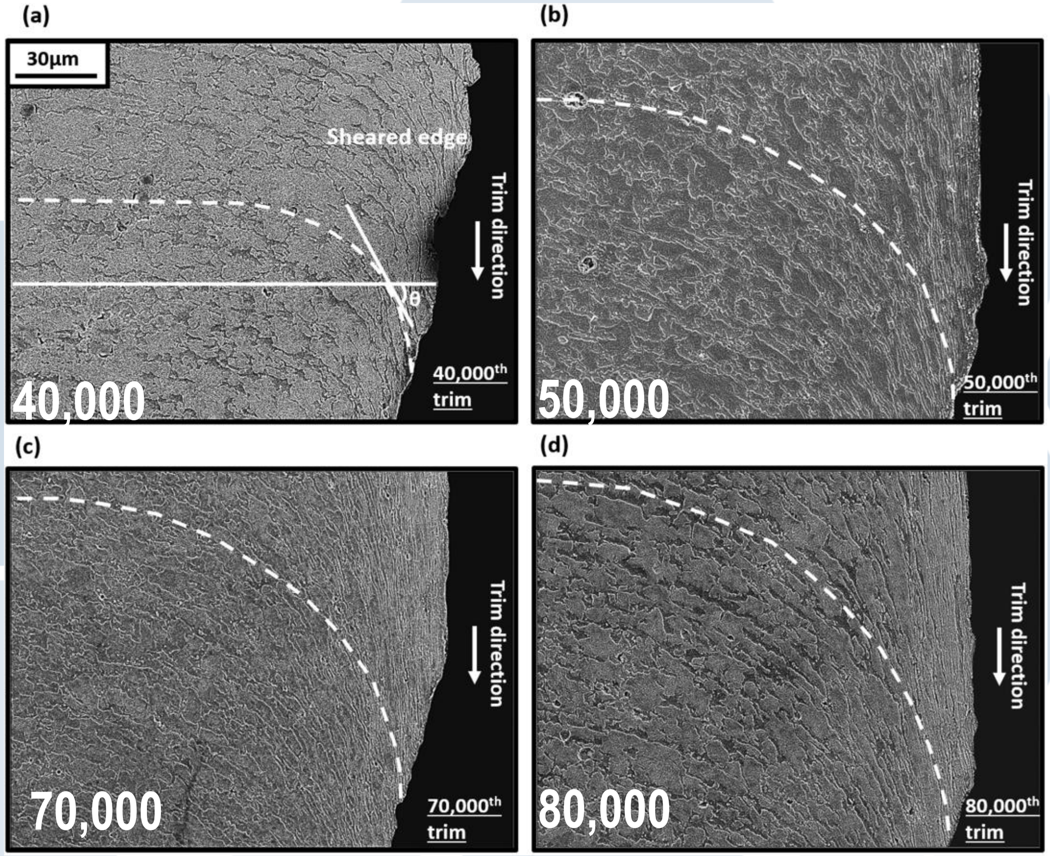

Cross-sectional SE-SEM images of DP980 parts obtained after (a) 40,000, (b) 50,000, (c) 70,000, and (d) 80,000 trimming cycles showing bending of martensite islands towards the trimming direction. A shear angle θ = 67° is shown in (a) indicating γ = 2.35 at a depth of 15 µm.

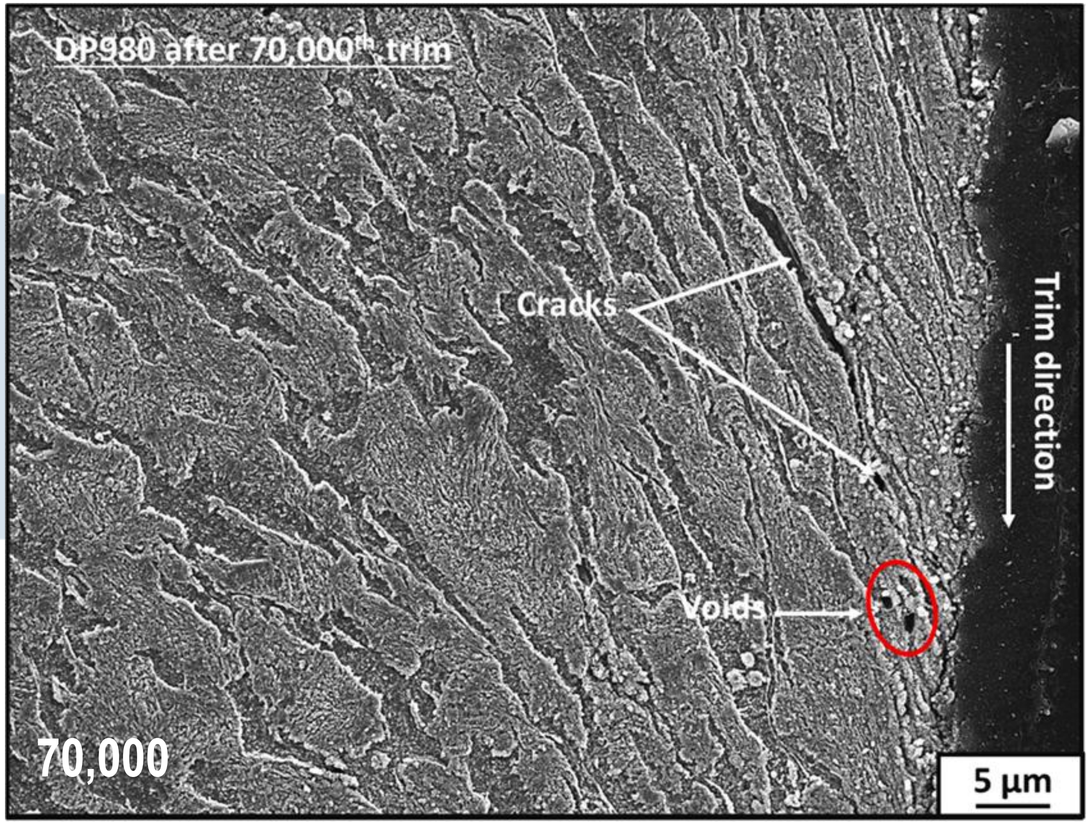

A cross-sectional SE-SEM image of a portion of the Shear Affected Zone of DP980 sheets obtained after 70,000 trimming cycles. Crack initiation at martensite/ferrite interfaces and void formations are observed close to the trimmed edge.

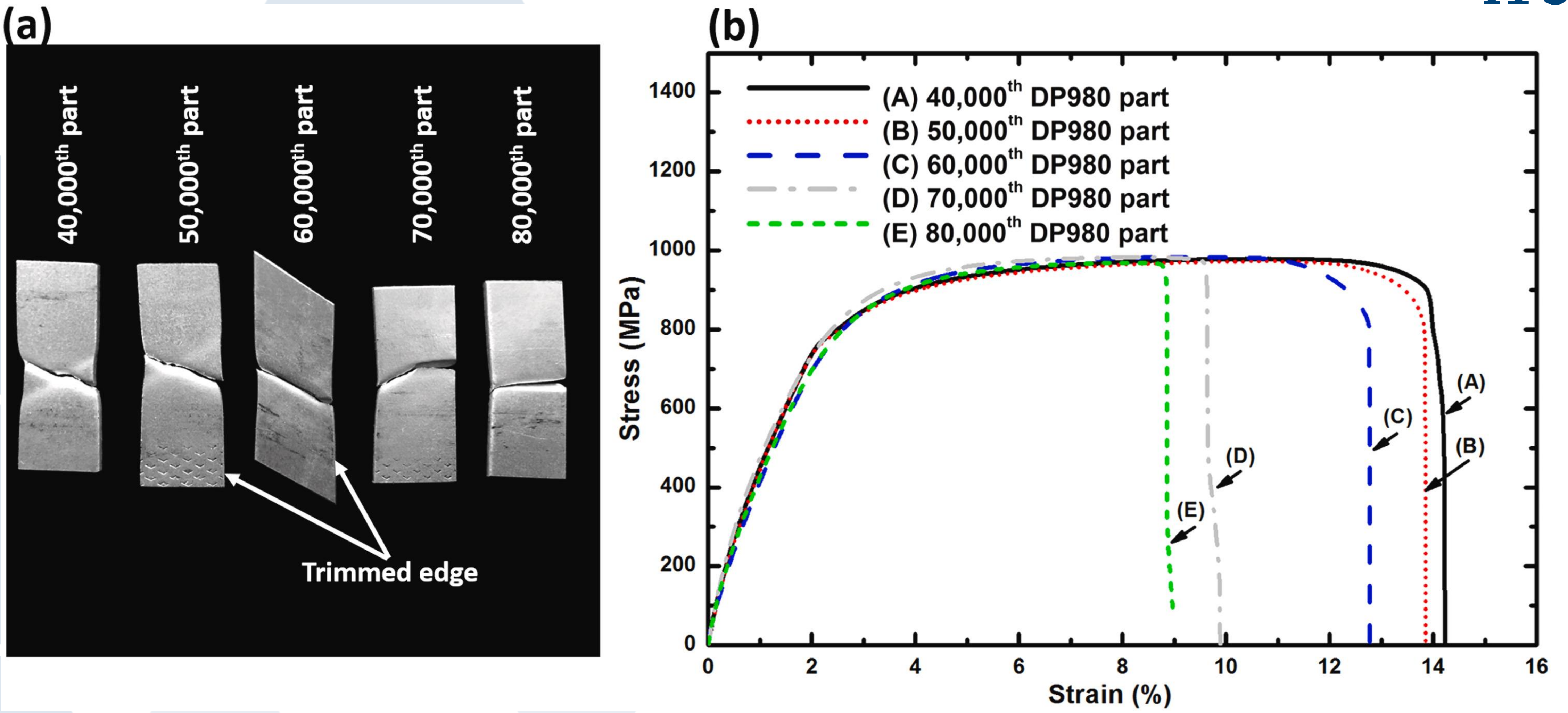

(a) Failure modes and (b) tensile stress-strain curves of trimmed DP980 sheets obtained after different trimming cycles.

Problem: Extending trimming cycle of the dies to reduce the risk of die wear induced tensile ductily loss of trimmed sheets from the perspective of the die material.

Approach: Understanding the progress of wear on D2 steels under impact-sliding contact and determine the role of microstructural constituenets on wear

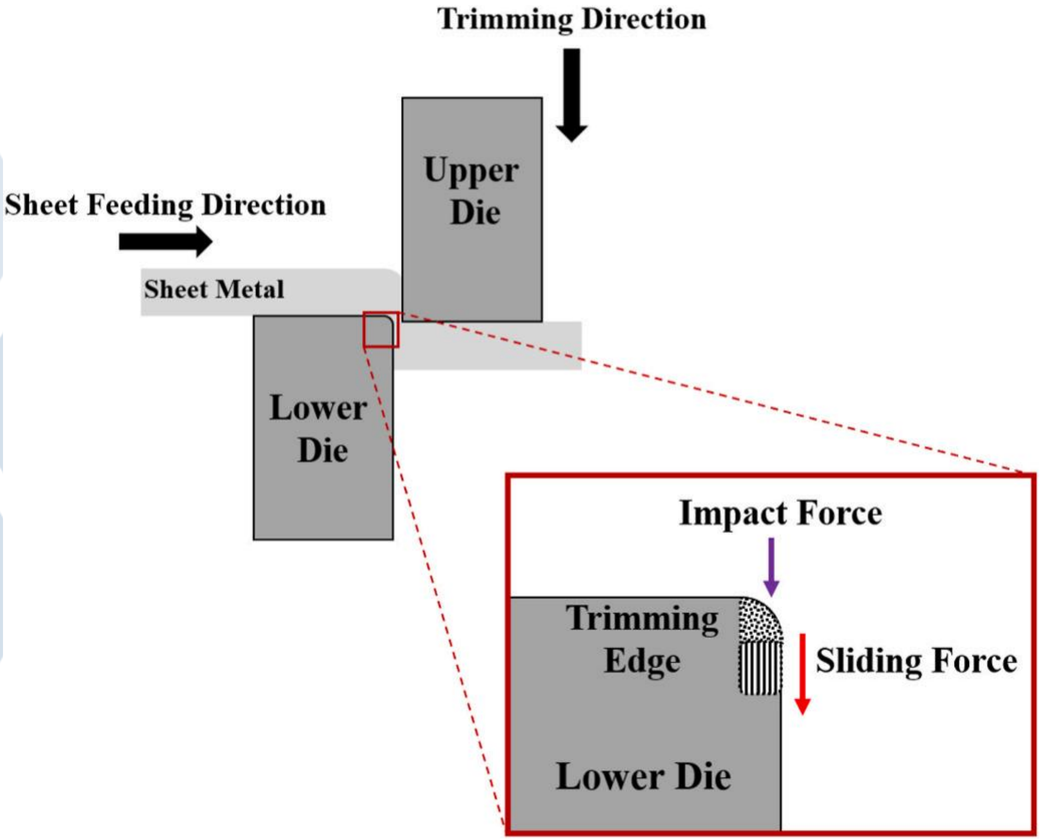

Schematic diagram of the trimming operation showing impact and sliding forces and the affected zones at the trimming edge of the lower die

Wear 538-539 (2024) 205224

ELSEVIER

Contents lists available at ScienceDirect

Wear

journal homepage: www.elsevier.com/locate/wear

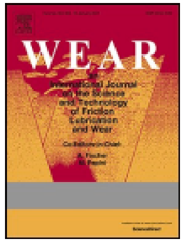

Check for updates

Microstructural effects on impact-sliding wear mechanisms in D2 steels: The roles of matrix hardness and carbide characteristics

M. Kaba [a], H.I. Filiz [a], Z. Cui [b], M. Baydogan [a], H. Cimenoglu [a], A.T. Alpas [b,*]

[a] *Department of Metallurgical and Materials Engineering, Istanbul Technical University, Istanbul, Turkey*
[b] *Tribology of Materials Research Centre, Department of Mechanical, Automotive and Materials Engineering, University of Windsor, Windsor, Ontario, Canada*

ARTICLE INFO

Keywords:
D2 cold work steel
Impact-sliding
Delamination wear
Carbide fracture
Chipping

ABSTRACT

This study investigates the wear micromechanisms of D2 steels under impact-sliding conditions, offering insights into their performance when used in applications such as trimming dies for high-strength steel sheets where they undergo plastic deformation and chipping. Two D2 steel samples, both with a bulk hardness of 59.7 HRC but different matrix hardnesses and carbide distributions, are tested by using an impact-sliding wear test rig at Hertzian contact pressures exceeding 2 GPa. The sample with a softer matrix exhibits wear primarily through delamination caused by plastic deformation. This initiates cracks at the matrix/primary carbide interface, leading to material loss in the form of large chips. In contrast, the steel with a harder matrix shows reduced wear due to its resistance to plastic deformation. Initially, wear occurs through the fracture of primary carbides. However, with prolonged loading, the matrix begins to soften, adopting a wear mechanism similar to the D2 steel with softer matrix. Notably, smaller primary carbides are associated with improved wear resistance by limiting the initiation sites for cracks, especially at the matrix/primary carbide interface. This understanding enables the selection and design of heat treatments to optimize D2 steel microstructure, thus improving resistance to impact-sliding wear damages observed in processes like trimming.

Chemical compositions of the D2 Steel Samples D2-A and D2-B.

Steel Code	C (wt. %)	Mn (wt. %)	P (wt. %)	S (wt. %)	Si (wt. %)	Cr (wt. %)	V (wt. %)	Mo (wt. %)
D2-A	1.49	0.26	0.02	0.001	0.32	11.27	0.78	0.73
D2-B	1.47	0.41	0.02	0.001	0.32	11.25	0.84	0.90

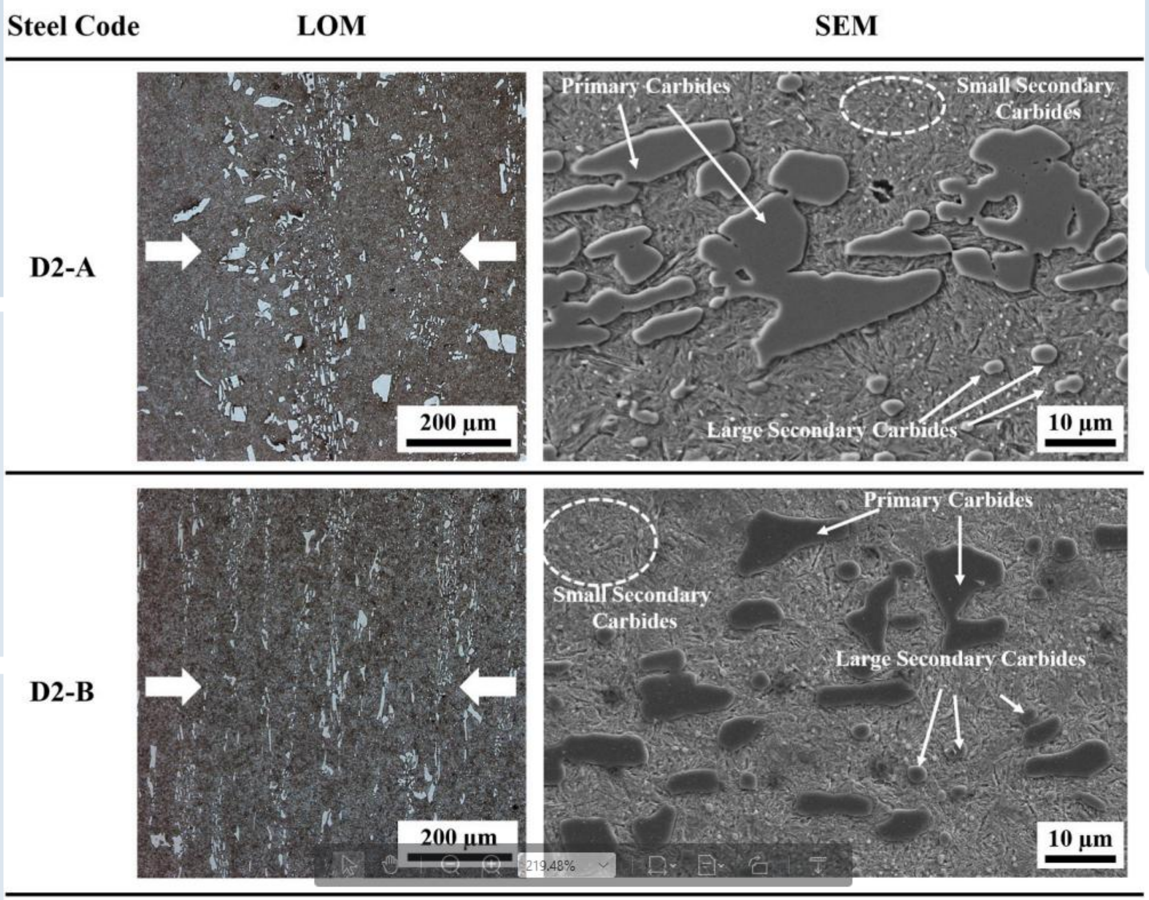

Bulk hardness of steels: 59.7 HRC

Matrix:Tempered martensite

Type of Carbides: M_7C_3 and $M_{23}C_6$,

Primary carbides : >5 μm

Secondary carbides: 1–5 μm

Small secondary carbides: <1 μm

Average carbide volume fractions and matrix hardness values of D2-A and D2-B steels.

Steel Code	Primary Carbides (vol. %)	Large Secondary Carbides (vol. %)	Small Secondary Carbides (vol. %)	Matrix Hardness ($HV_{0.025}$)
D2-A	9.6 ± 0.8	2.2 ± 0.1	0.3 ± 0.05	595 ± 37
D2-B	6.2 ± 0.5	3.9 ± 0.2	0.4 ± 0.07	710 ± 20

Impact Sliding Wear Tests

The maximum loads: 75 N (impact) and 300 N (sliding)

Loading cycles: 500, 1000 and 2000

Loading frequency: 2.5 Hz

Counterface: 10 mm dia 52100 grade bearing steel ball (~850 HV).

Test temperature: RT

Max. Hertzian contact pressure acting to impact and sliding zones were 2.0 and 3.2 GPa, respectively

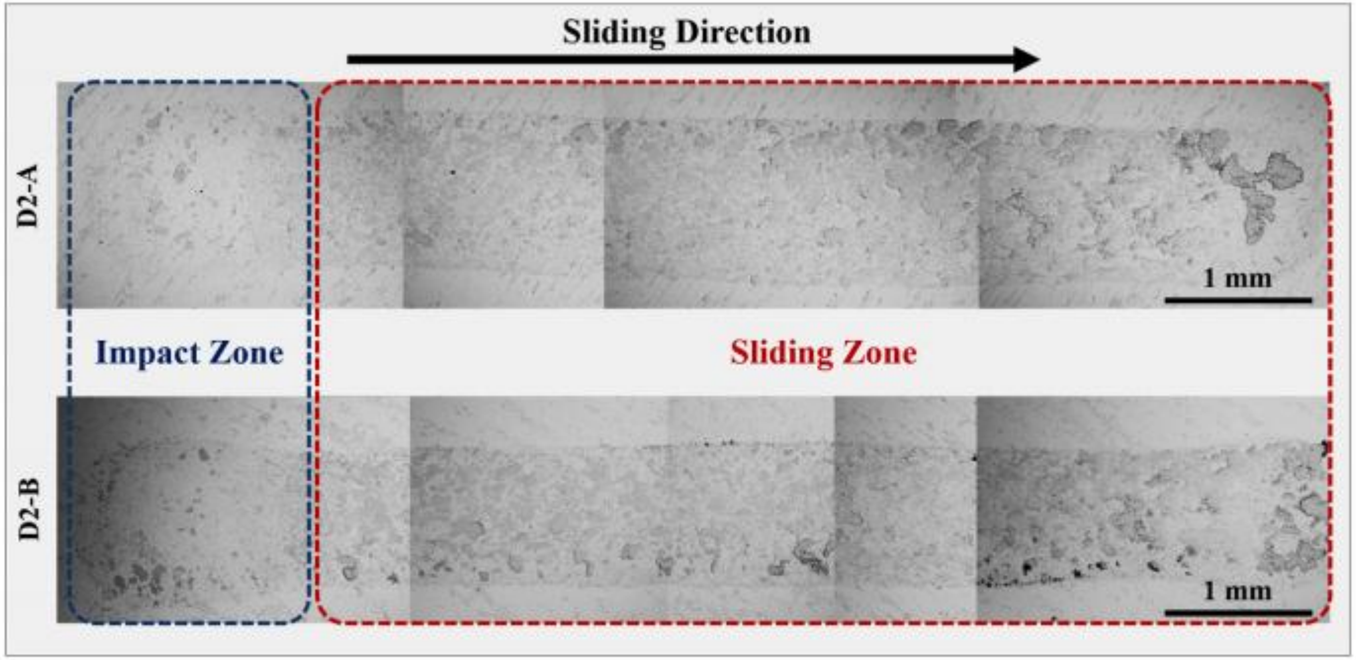

(a)

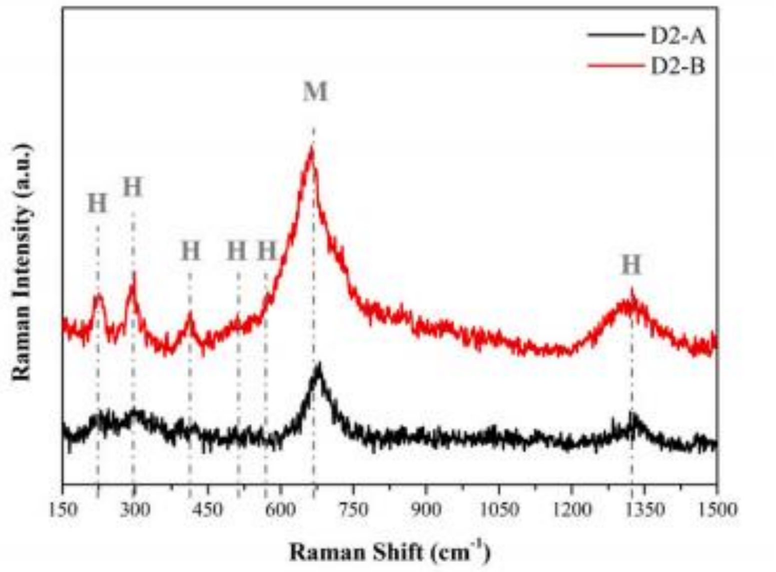

(b)

Low magnification SEM images of the wear tracks formed on the D2-A and D2-B steels each with a total length of ~8.5 mm after 2000 impact-sliding loading cycles, showing both impact and sliding zones. The sliding direction is shown by an arrow. (b) Raman spectra of the tribo-oxides detected on the sliding zone of the wear tracks (H: Hematite and M: Magnetite).

Worn Surface and Cross-section Examinations
D2A Steel

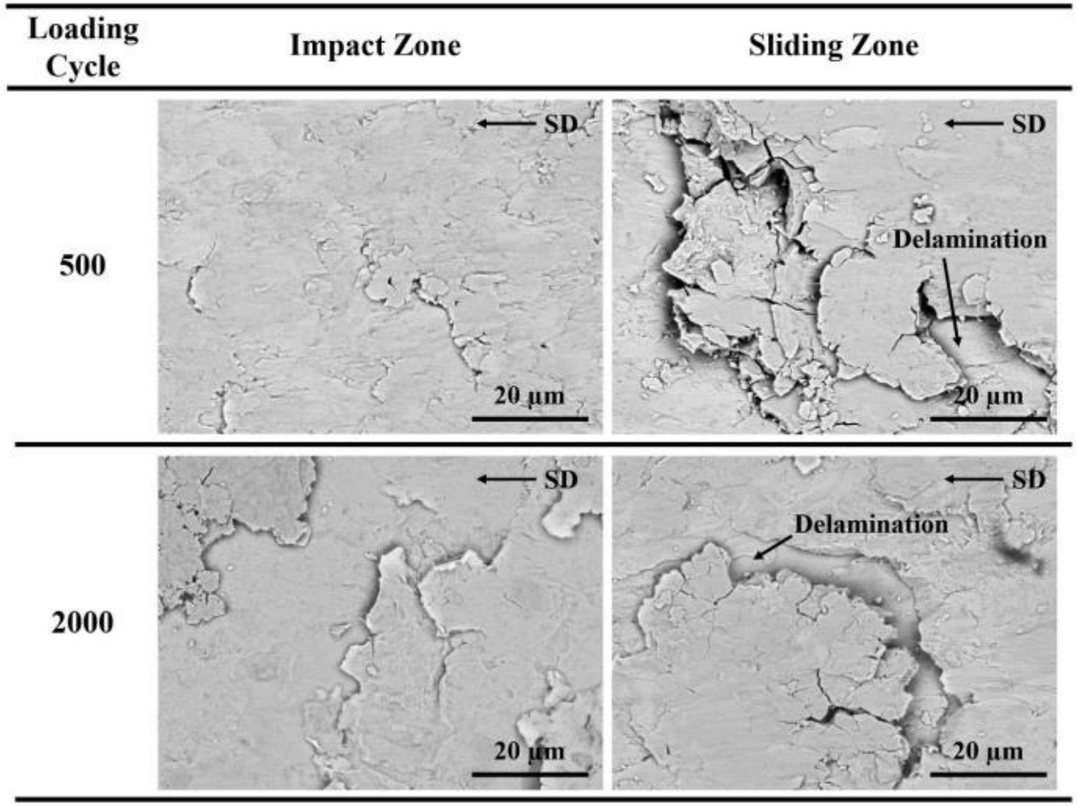

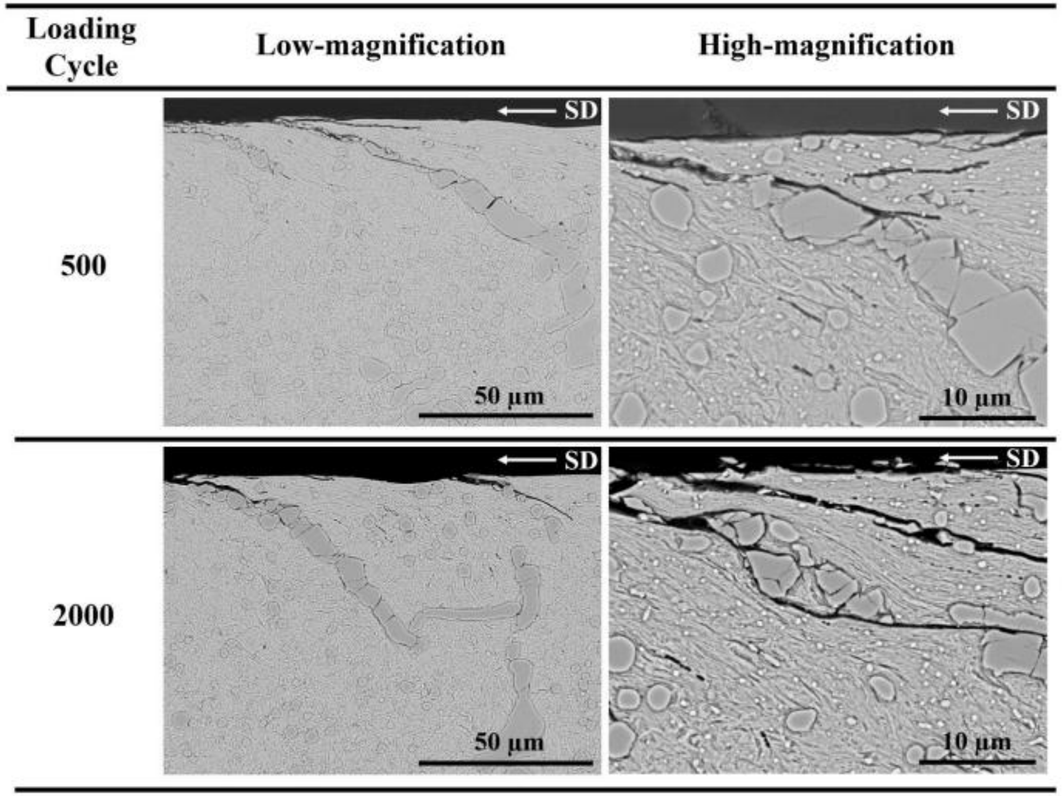

D2-A steels with relatively lower hardness, wear was induced by plastic deformation, characterized by crack initiation and propagation along the interfaces of the matrix and primary carbides within the plastically deformed region under the wear track.

Worn Surface and Cross-section Examinations
D2B Steel

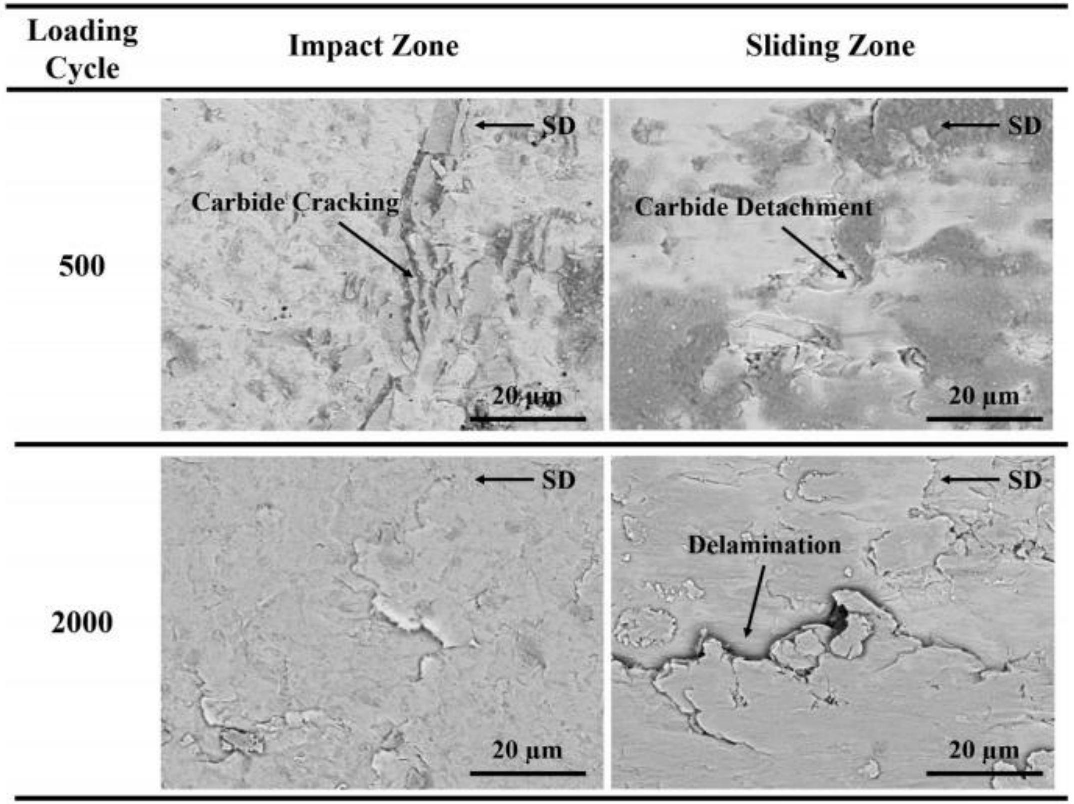

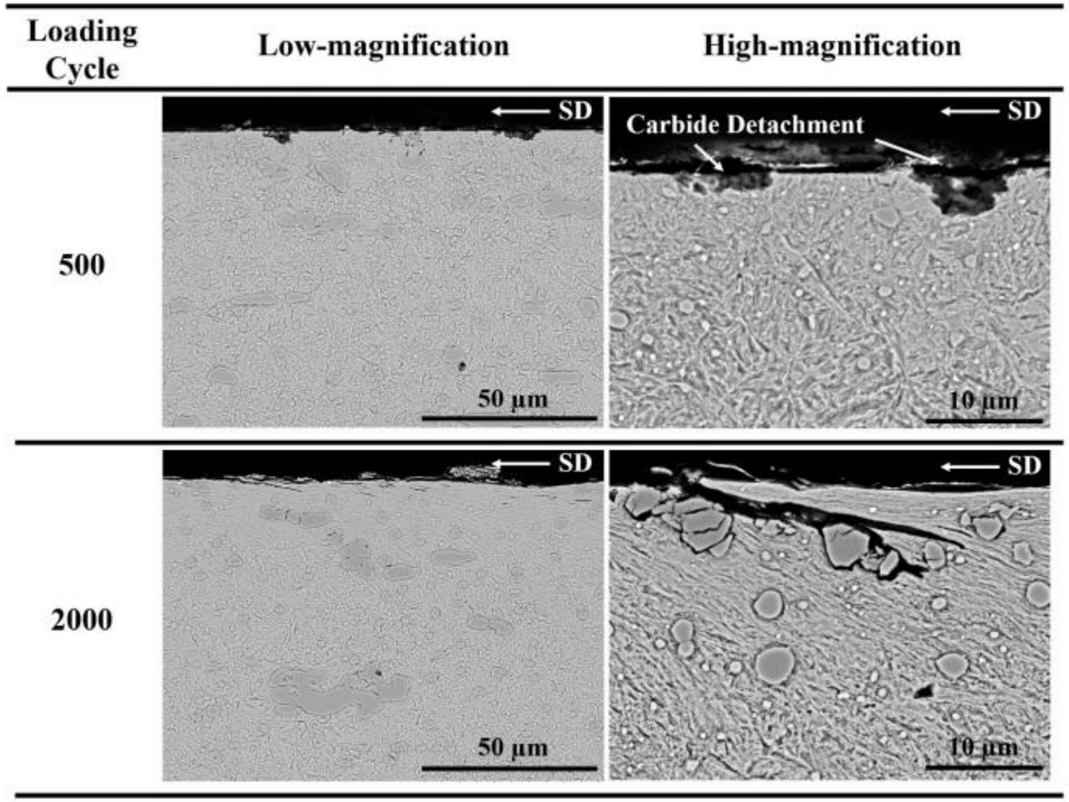

Higher matrix hardness in D2-B steel provided greater resistance against plastic deformation on the contact surface. Wear initially occurred by surface carbide cracking and removal, but in plastic deformation-induced wear caused delamination and chip formation at higher loading cycles. The smaller size of the primary carbides contributed to wear resistance by reducing the number of sites prone to easy crack initiation

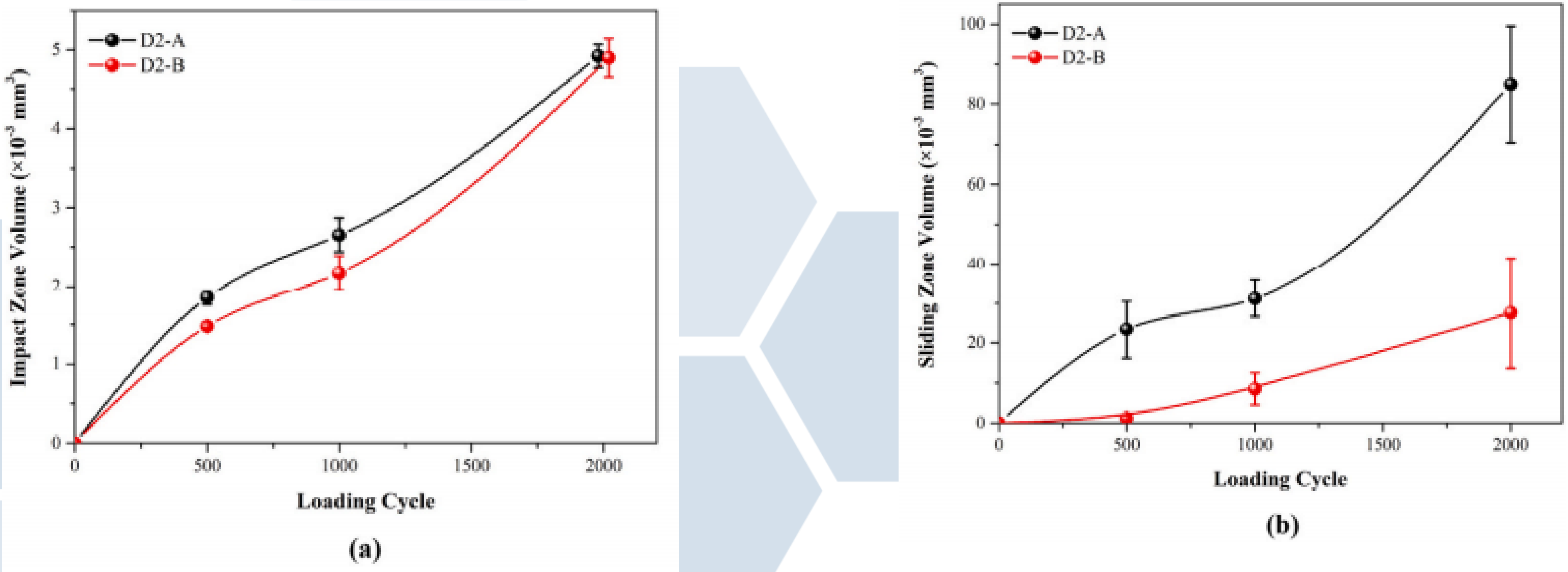

Increases in the average volumes of (a) impact and (b) sliding zones of the wear tracks formed on D2 steels with the loading cycles.

Conclusion:

The D2 steel having smaller primary carbides and higher matrix hardness exhibits better wear reisistance under impact -sliding contact.

Wear mechanism of D2-B steel at low and high cycles.

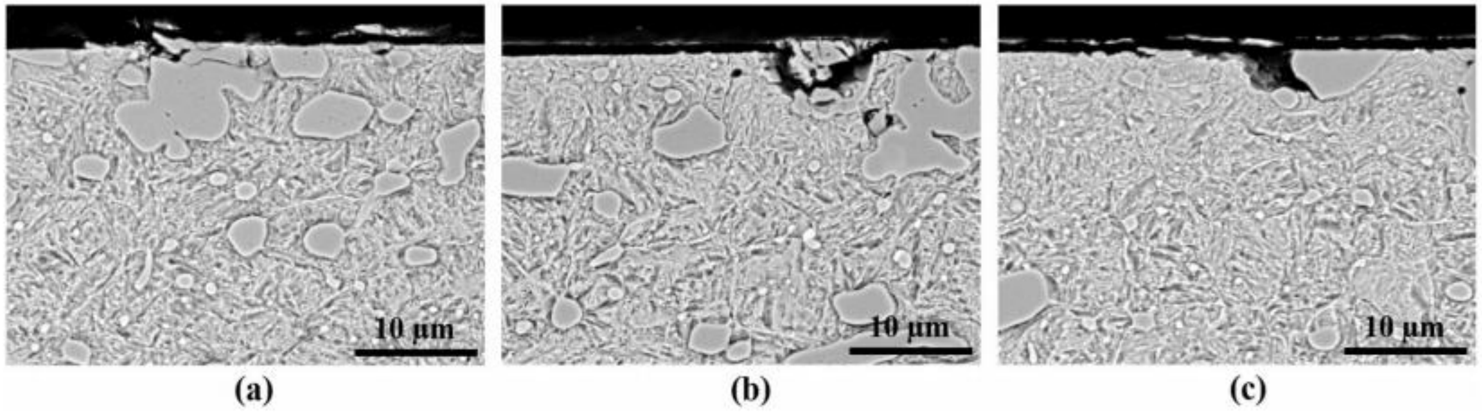

Fig. 12. Progression of wear through carbide fracture (in the absence of severe subsurface plastic deformation) shown in the sequence of (a) cracking, (b) fragmentation and (c) detachment of primary carbides (SEM images taken from the cross-sections of the D2-B steels tested for 500 cycles).

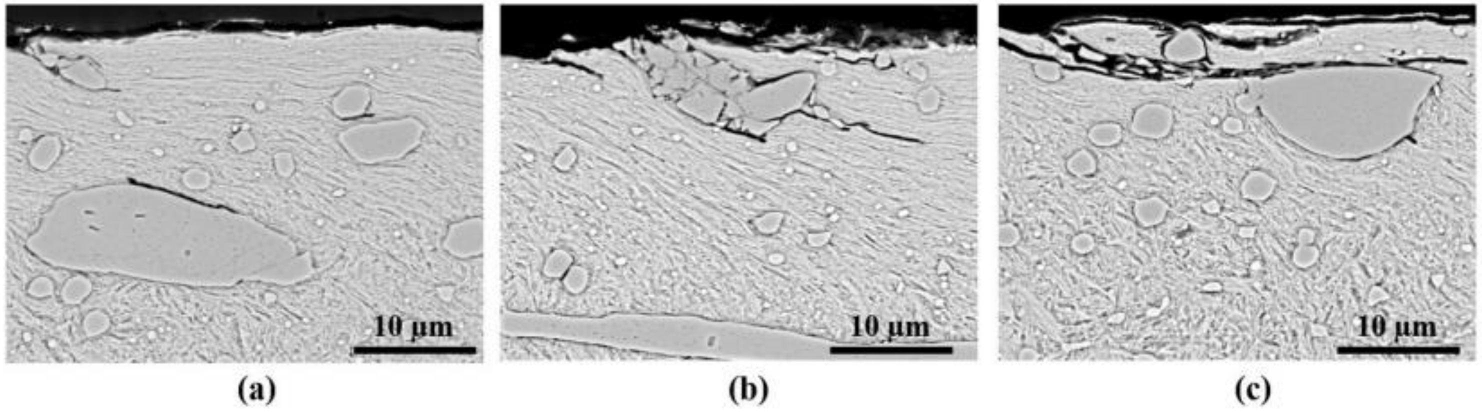

Fig. 13. Progression of plastic deformation induced wear by delamination shown in the sequence of (a) initial cracking and (b, c) crack propagation at primary carbide/matrix interface after severe subsurface plastic deformation of the matrix. (SEM images were taken from the cross-sections of the D2-B steels tested for 2000 cycles).

Conclusion

Laboratory scale impact-sliding wear tests that simulate the the loading conditions of metal forming dies have potential to offer technological solutions for extending die lives quickly and cheaply. Therefore it can be classified as; “simplified component test”

From scientific perspective impact-sliding wear tester has potential to investigate wear behaviours of materials targeted to be used under heavy and complex loading conditions.

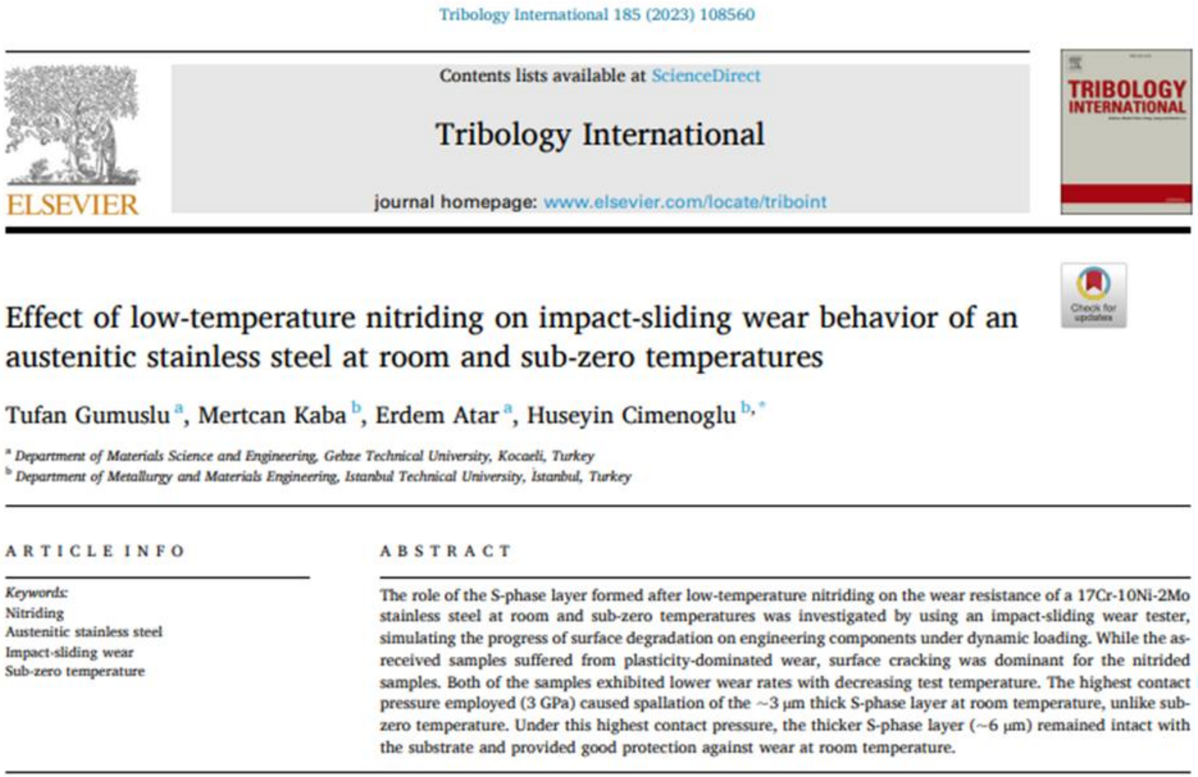

Tribology International 185 (2023) 108560

Contents lists available at ScienceDirect

Tribology International

journal homepage: www.elsevier.com/locate/triboint

Effect of low-temperature nitriding on impact-sliding wear behavior of an austenitic stainless steel at room and sub-zero temperatures

Tufan Gumuslu [a], Mertcan Kaba [b], Erdem Atar [a], Huseyin Cimenoglu [b,*]

[a] Department of Materials Science and Engineering, Gebze Technical University, Kocaeli, Turkey
[b] Department of Metallurgy and Materials Engineering, Istanbul Technical University, Istanbul, Turkey

ARTICLE INFO

Keywords:
Nitriding
Austenitic stainless steel
Impact-sliding wear
Sub-zero temperature

ABSTRACT

The role of the S-phase layer formed after low-temperature nitriding on the wear resistance of a 17Cr-10Ni-2Mo stainless steel at room and sub-zero temperatures was investigated by using an impact-sliding wear tester, simulating the progress of surface degradation on engineering components under dynamic loading. While the as-received samples suffered from plasticity-dominated wear, surface cracking was dominant for the nitrided samples. Both of the samples exhibited lower wear rates with decreasing test temperature. The highest contact pressure employed (3 GPa) caused spallation of the ~3 μm thick S-phase layer at room temperature, unlike sub-zero temperature. Under this highest contact pressure, the thicker S-phase layer (~6 μm) remained intact with the substrate and provided good protection against wear at room temperature.

Motivation :

SZT application areas of ASSs include pipelines and transportation systems for liquid nitrogen, liquid oxygen and hydrogen storage in rocket engines, superconducting magnets, hydraulic parts, offshore lifting devices, bolting materials, pressure vessels, flanges, fittings, turbo-pump bearings, valves, heat exchanger parts, marine hardware, submarine, refrigeration for material processing and food storage, etc.

30X" cold-rolled stainless steel is a proprietary, ultra-hard, and corrosion-resistant alloy developed by SpaceX and used for the Tesla Cybertruck. . This alloy, derived from the 300-series stainless steel, offers a significant increase in strength due to its microstructure, which includes both austenite and martensite formed through cold rolling. This enhances the Cybertruck’s ability to withstand impacts and resist dents, making it incredibly durable compared to conventional truck materials.

Features of the S-Phase

316 L grade ASS nitrided at 420 ◦ C for 4 h in a fluidized bed reactor containing alumina particles as the gas and heat carriers.
The nitriding atmosphere was a mixture of 60% NH 3 and 40% N 2 .

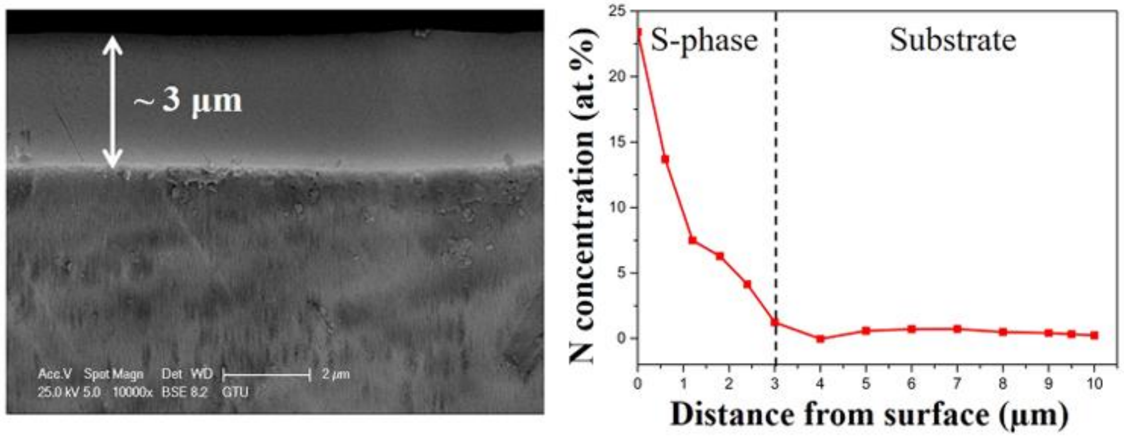

(a) (b)

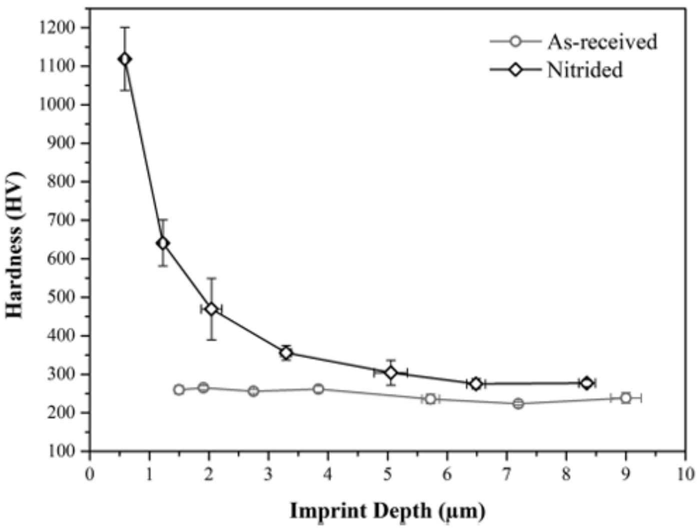

RT

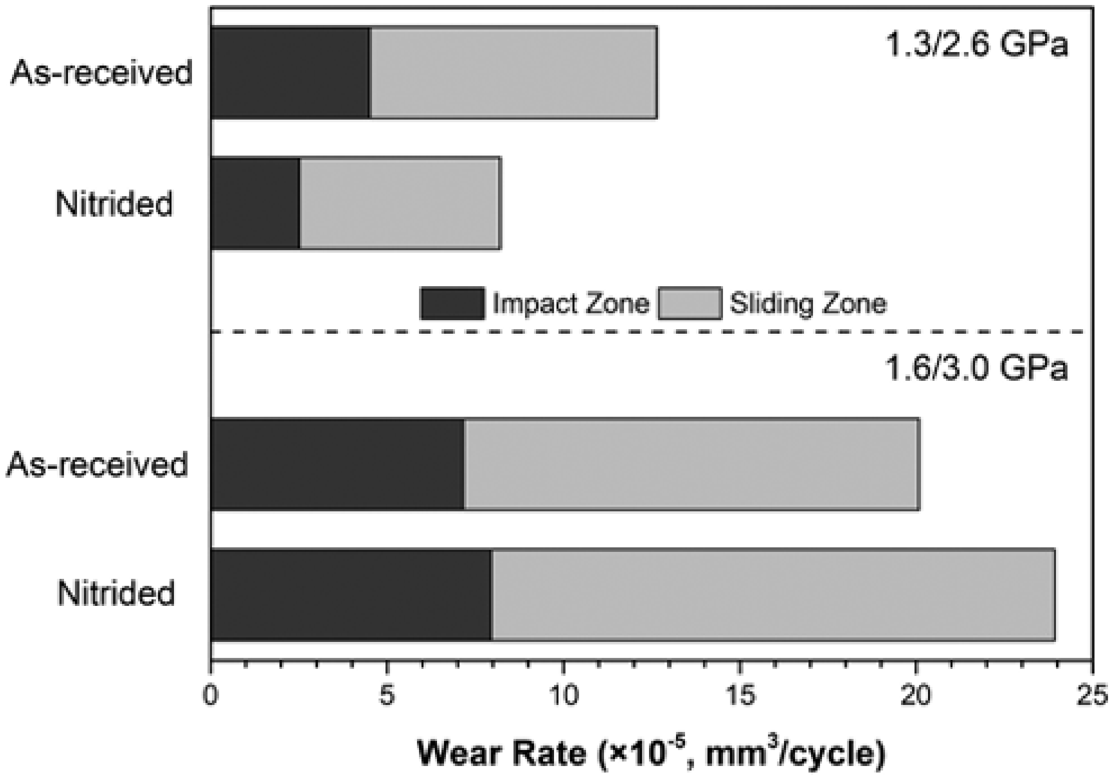

SZT

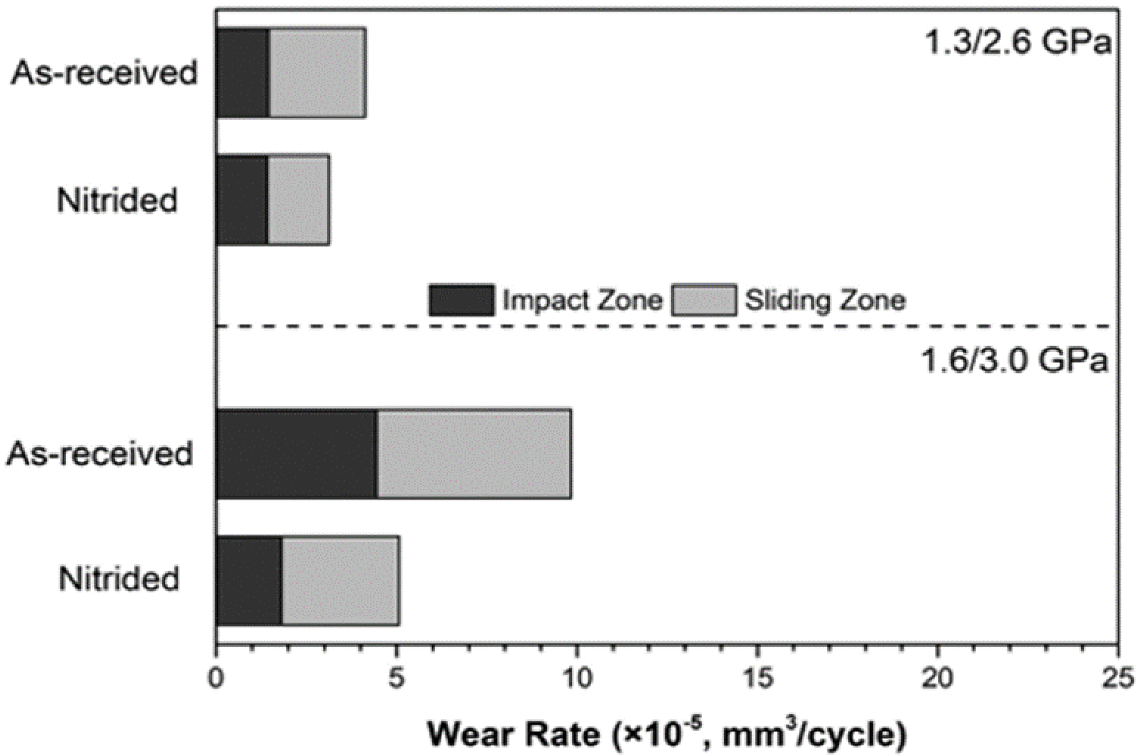

Wear rates of the as-received and nitrided samples tested at RT and SZT

Wear of as-received alloy

RT

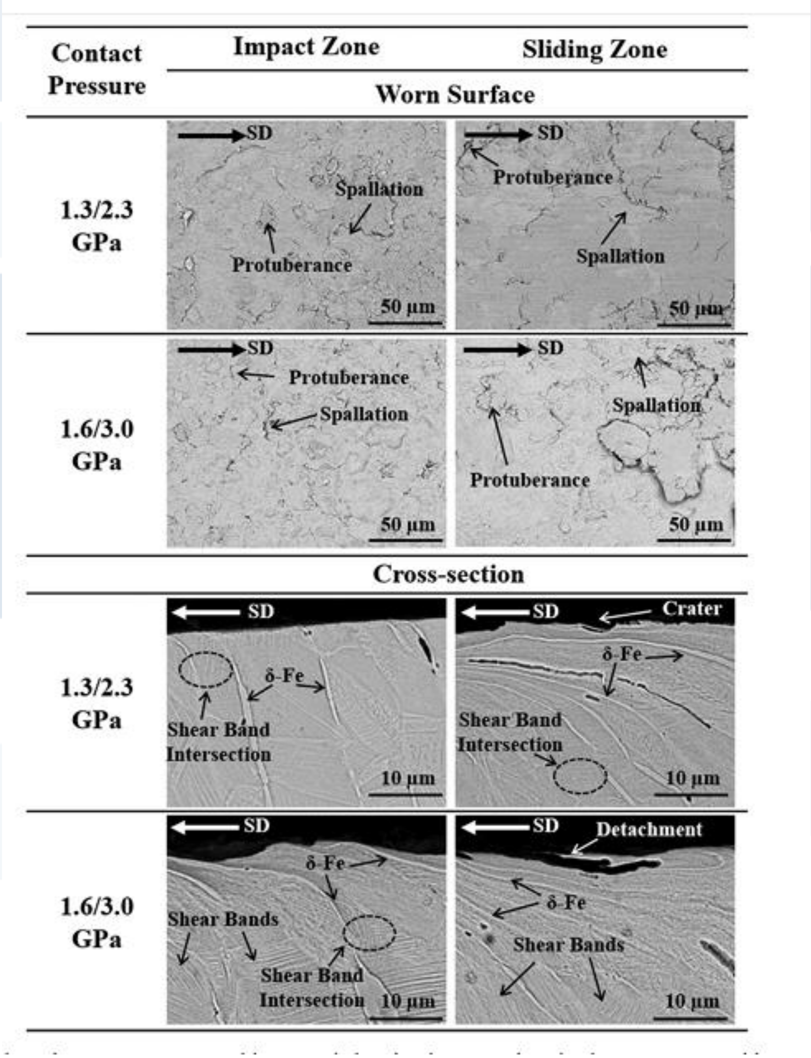

SZT

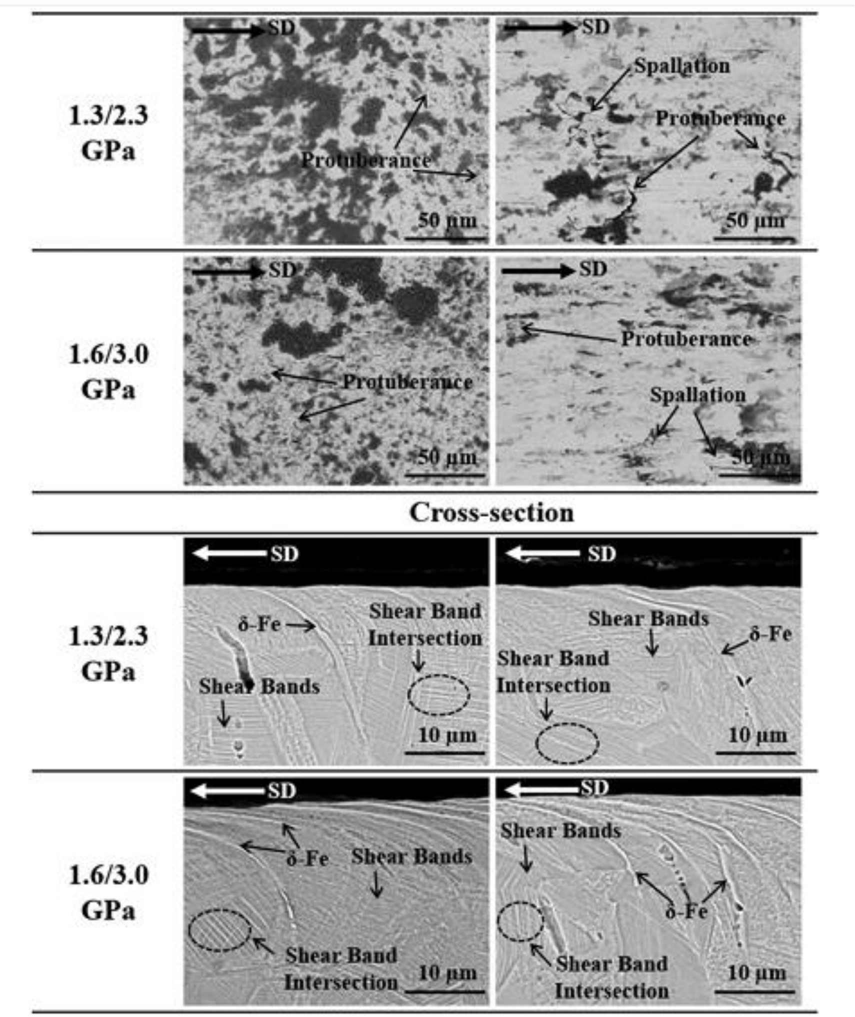

Wear of nitrided alloy

RT

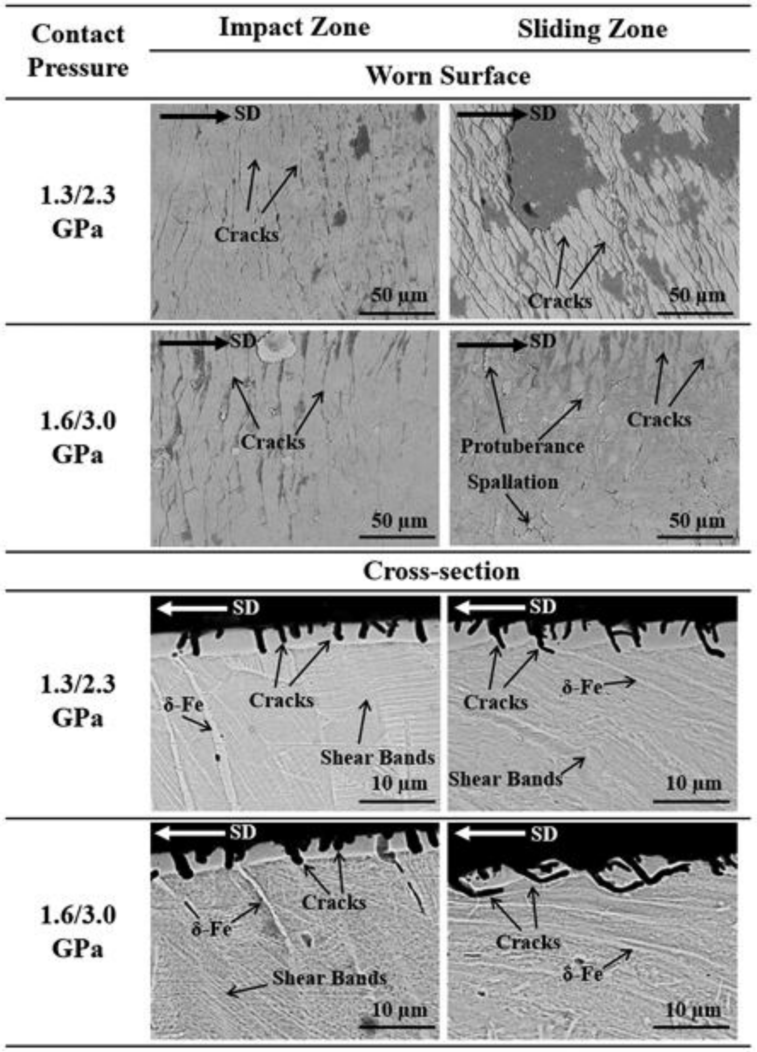

SZT

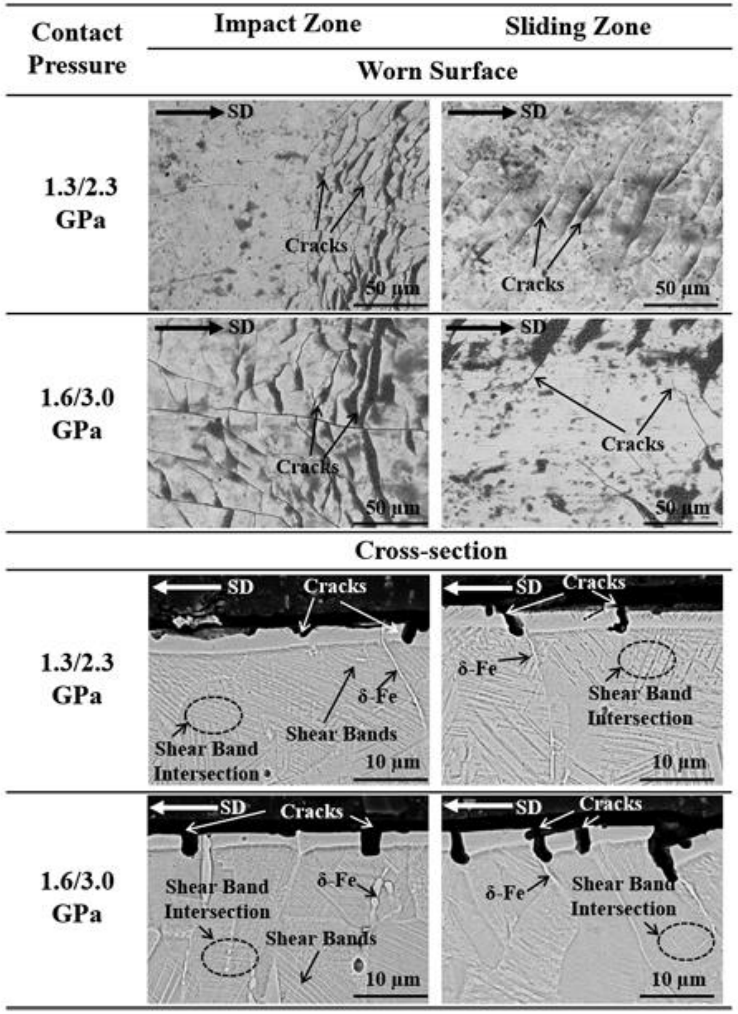

Conclusion

The decrease of test temperature from RT to SZT and/or contact pressure set from 1.6/3.0 GPa to 1.3/2.3 GPa was accompanied by a reduction in wear rate for both as-received and nitrided samples.

Under the contact pressure set of 1.3/2.3 GPa, nitrided samples exhibited 35% and 25% lower wear rate than as-received samples at RT and SZT, respectively.

The contact pressure set of 1.6/3.0 GPa caused the nitrided sample to exhibit a 15% higher wear rate than the as-received sample at RT due to gross spallation of the S-phase layer. At SZT the nitrided sample possessed a 50% lower wear rate as

Acknowledgements

Ahmet Alpas, PhD

Murat Baydoğan, PhD

Erdem Atar, PhD

Faiz Muhaffel, PhD

Seçkin Özkurt, MSc

Mert Altay, PhD

Mertcan Kaba, MSc

Ezgi Akyıldız, MSc

Tufan Gümüşlü, MSc

H.İbrahim Filiz, MSc

Zeyuan Cui, PhD

KTU 1955 KARADENIZ TECHNICAL UNIVERSITY

TECHNISCHE UNIVERSITÄT CHEMNITZ

Sumela Monastery

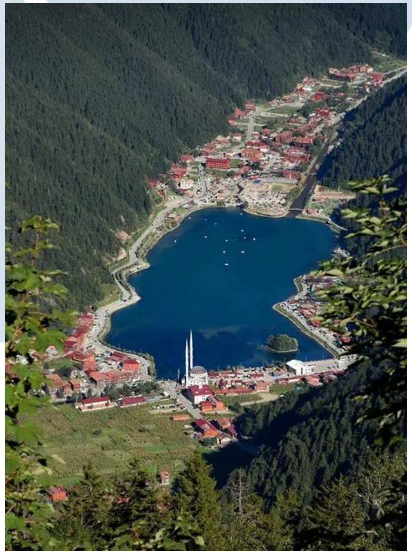

Uzungöl (Long Lake)

IMPORTANT DATES

- Early bird registration due : June 30, 2026
- Deadline for submission of abstracts : August 31, 2026
- Notification of acceptance for abstract : September 15, 2026
- Deadline for submission for full paper : September 30, 2026
- Final acceptance for full paper : October 15, 2026
- Program available online : October 1, 2026
- **Conference Dates : November 4-7, 2026**

More information;
https://www.tribosurf.com/